UNIVERSITÄTSKLINIKUM HAMBURG-EPPENDORF

Department of Osteology and Biomechanics

Heisenberg Research Group
AG Bioengineering
Group leader: Prof. Dr. rer. medic. Björn Busse

Director: Prof. Dr. med. Michael Amling

Ex situ analysis of bone mineral density and cellular activity in type 1 diabetes mellitus

Dissertation

zur Erlangung des Grades eines Doktors der Medizin
an der Medizinischen Fakultät der Universität Hamburg.

vorgelegt von:

Ma Liangyu

aus Xining, China

Hamburg 2020

Angenommen von der
Medizinischen Fakultät der Universität Hamburg am: 26.10.2020

Veröffentlicht mit Genehmigung der
Medizinischen Fakultät der Universität Hamburg.

Prüfungsausschuss, der/die Vorsitzende: Prof. Dr. Franz Rinninger

Prüfungsausschuss, 2. Gutachter/in: Prof. Dr. Björn Busse

Contents

1. Abstract……..1

2. Introduction……..……2

2.1 Human bone ……..……..……...…2

2.1.1 Vertebra and femur……..…2

2.1.2 Bone micro- and nanostructure……..……..……..…4

2.1.3 Bone cells……..…5

2.1.4 Bone turnover mechanism……..…7

2.2 Diabetes Mellitus…….……..…..……8

2.3 Dual-energy X-ray absorptiometry and bone mineral density…….....10

2.4 Purpose of this study…….……..……11

2.5 Hypothesis……11

3. Material and methods……13

3.1 Sample collection……..…13

3.2 DXA measurement……..……...14

3.3 Embedding, grinding, and staining……...14

3.4 Histomorphometry analysis……16

3.4.1 Thin section……..……..…….16

3.4.2 Ground section……..…….18

3.5 Statistical analysis…….……..19

4. Results……20

4.1 DXA results of bone mineral density…….……..20

4.2 Histomorphometry results…….……..23

4.2.1 Histological section……..……..……..23

4.2.2 Ground section…..……..……..……..27

4.2.3 Comparison between thin and ground sections……..…..……..30

5. Discussion……..……32

5.1 Bone mineral density and cellular activity in T1DM.……..32

5.2 Concluding hypothesis.……..……..34

5.3 Strength of the study……..……..34
5.4 Limitation of the study……..……..36
5.5 Outlook……..36

6. Summary……..……..38
6.1 Summary (English version)……..……...38
6.2 Zusammenfassung (Deutsche Version)……..……..39

7. Abbreviation……40

8. Appendix……..……..41

9. References……42

10. Acknowledgements……..……..…52

11. Curriculum Vitae……..……..53

12. Affidavit (Eidesstattliche Erklärung)……..……..…..54

1. Abstract

Type 1 diabetes mellitus (T1DM) - characterized by insulin deficiency - affects 20-40 million individuals worldwide. A 6-fold higher incidence of hip fracture is seen in patients compared to non-diabetic individuals. Studies of bone mineral density (BMD) in T1DM are controversial obscuring fracture risk assessment. Changes in bone turnover by altered remodelling activities of bone-resorbing osteoclasts and bone-forming osteoblasts will affect bone quality indices and may impair fracture characteristics. This study aims to analyse BMD and cellular indices of bone turnover of individuals affected by T1DM.

Femoral cortices of the mid-diaphysis from 14 individuals (7 Control and 7 T1DM, 47.29±5.12 and 48±7.68 years) and the 11th thoracic to 1st lumbar vertebrae from 28 individuals (19 Control and 9 T1DM, 47.11±4.98 and 48.67±6.5 years) were obtained during autopsy after Institutional Review Board (IRB) approval. Vertebral BMD was determined by applying dual-energy X-ray absorptiometry (DXA) while cellular indices were analysed via histomorphometry in the anterior quadrant of the femoral cross-section (divided into endo-, intra-, and peri-cortical region).

DXA result shows that equal BMD is found in 12th thoracic - 1st lumbar vertebrae in Control and T1DM groups. Histomorphometry reveals higher eroded surface per bone surface in T1DM than Control group (17.957±3.389 % vs 8.390±5.223 %, p=0.036). While osteocyte number in endo-cortical region is lower in T1DM compared to Control group (43.555±13.075 #/mm^2 vs 63.874±16.208 #/mm^2, p=0.035).

Our results link the quantified values for BMD to cellular activity in healthy individuals and individuals afflicted with T1DM. In contrast to the femoral neck as common skeletal fracture site, the femoral mid-diaphysis is predominantly composed of cortical bone presenting with higher resorption activity in T1DM compared to non-diabetic Control group. Furthermore, all individuals have been on insulin treatment which might potentially have bone-anabolic effects and thus interfere with fracture risk.

2. Introduction

2.1 Human bone

The human skeleton, composed of the axial and the appendicular skeleton, is the internal framework of the body and has multiple functions. Two major functions of bone are i) to ensure mechanical integrity for locomotion and protection, and ii) to ensure the body's mineral metabolism [1]. Bones are composed of the outer compact shell, also called cortical bone, and inner trabecular bone [2]. Cortical bone accounts for 80% of the weight of the skeleton and has a higher density and stiffness than trabecular bone which only takes up 20% of the skeleton [3]. The calcium content is lower in trabecular bone compared to cortical bone while the water content is higher [4]. However, trabecular bone has a larger surface area and is more active in bone metabolism than compact cortical bone [5]. The outer cortical bone mainly provides strength for long bones such as the femur while the inner trabecular bone mainly distributed in epiphysis or vertebrae is for load transferring [6]. Both cortical and trabecular bone contribute to failure loading of proximal femur as shown in an *ex vivo* study [7]. The composition of cortical and trabecular bone at each individual skeletal site are dependent on the function of the individual bone.

2.1.1 Vertebra and femur

According to different regions and positions, vertebrae can be categorized as 7 cervical spine vertebrae, 12 thoracic spine vertebrae and 5 lumbar spine vertebrae, sacrum and coccyx, together making up the entire spine. Vertebrae are a common fracture site in patients with osteoporosis [8]. A vertebra is composed of the vertebral body, vertebral arch (Lamina and Pedicle), transverse process, and spinous process (Figure 1 A Superior View). The vertebral body, which contains inner cancellous bone covered by outer compact bone (Figure 1 A Lateral View), are connected to each other by intervertebral discs and ligaments. The endplates of the vertebrae connect directly with intervertebral discs which form joints for load transfer and nucleus pulpous protection. In vertebrae, cortical bone is a protective layer known as the dense outer

coating surface. The thickness of cortical bone is ranging from 180 to 600 μm with a mean value of 380 μm [9-12]. Trabecular bone predominates to resist compressive forces and its quality is essential for the performance of the whole spine [13]. Trabecular bone in the vertebral body has an inhomogeneous microstructure distribution [14]. The posterior region has a higher bone volume fraction than the related central and anterosuperior regions [15]. Due to this property of trabecular heterogeneity, compression wedge fracture can often be seen in severe osteoporotic patients. Bone strength of vertebrae is determined by bone size, cortical thickness, trabecular density and microarchitecture [16]. Age related bone loss, which includes alterations in bone quantity, bone matrix composition, and microarchitectural changes, may lead to osteoporosis with increased fracture risk [17, 18]. The most frequent part of osteoporosis-related vertebral fractures is below the mid-thoracic region [19]. Different parameters, that are established for describing the microstructure of trabecular bone regarding the properties of individual trabeculae, might have different associations with age. For example, bone volume per total volume (BV/TV), trabecular number (Tb.N), and trabecular separation (Tb.Sp) of vertebrae are age-related while trabecular thickness (Tb.Th) has been shown to be affected differently by age-related changes [8, 20]. Previous studies concerning trabecular bone loss in the process of aging is mainly represented by reduced Tb.N compared to slightly reduced Tb.Th [21]. Apart from aging, other diseases such as renal osteopathy, diabetes mellitus, and inflammatory bowel disease can also result in trabecular microstructure and quality changes [22-27].

The femur is the longest and strongest bone in the human skeleton which is composed of a diaphysis and two epiphyses that connect with adjacent bones in the hip and knee. In the femur, cortical bone does not only resist compressive forces but also torsional forces that can support whole body weight during standing and movement. The femur diaphysis mainly contains cortical bone while the epiphyses contains both cortical and cancellous bone. The volume of cortical bone in femoral neck, which takes up one fourth of the total neck volume, corresponds to the volume of diaphyseal cortical bone [28]. However, femoral neck cortical bone has only half of the density comparing to diaphyseal cortical bone [23]. Compact cortical bone is primarily responsible for load bearing and force transmission [29], whereas trabecular bone builds a framework which supplies large surface to allow for minerals and growth factor supply [30]. Both compact cortical and spongy trabecular bone of the femoral

neck make significant contributions to the strength of the proximal femur [7]. The cross-sectional area and cortical bone thickness in the femoral diaphysis seem to decrease with age especially in females [31]. The decreasing bone mass and subsequent bone quality impairment may pose a growing burden on the function of the femur which possibly increases the relative risk of femur fracture. Thus, understanding the changes in bone microstructure and bone turnover might be helpful in prevention and treatment of disease-related bone fractures.

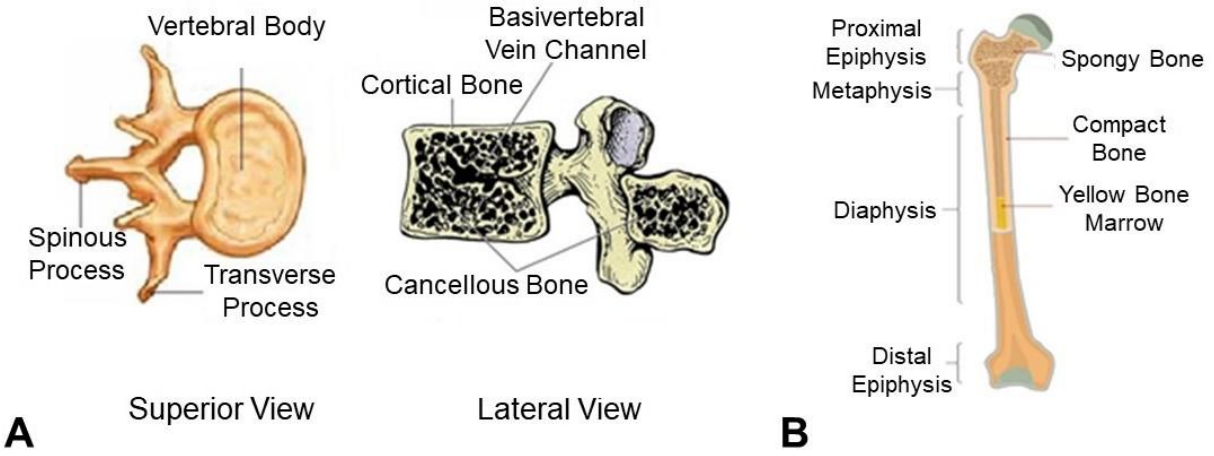

Figure 1. Lumbar vertebra and femur. (A) Superior view shows a vertebra composed of body, arch, spinous and transverse process; Lateral view of vertebra shows the outer compact cortical bone and inner cancellous/ trabecular bone. (B) Schematic diagram of a femur: the femur is composed of proximal and distal epiphysis, metaphysis, diaphysis. Trabecular bone is present in epiphysis and metaphysis however not in diaphysis, while yellow bone marrow can be seen in the medullary cavity (A is from [32, 33] and B is from [34]).

2.1.2 Bone micro- and nanostructure

At the tissue level of microstructure, cortical bone is composed of osteons, the basic structural units. Each osteon contains an inner Haversian canal, an outer cement line border and concentrically arranged lamellae within an osteon where osteocytes are embedded. Blood vessels and nerves are located in the Haversian canal and these vessels can supply the bone metabolism with nutrients and oxygen. The diameter of osteons is approximately 170 ~250 μm while the thickness of cement line and lamellae are about 5 μm [35-37].

At the nanostructure, bone is composed of carbonated hydroxyapatite nanoparticles and collagen-rich organic matrix [38]. Mineralized collagen fibrils, with a diameter of 50~200 nm, are the basic elements of bone material [38]. Collagen fibrils,

filled and coated by mineral crystallites, are constituted of type I collagen and have triple helices with 300 nm length that are assembled within cells [39].

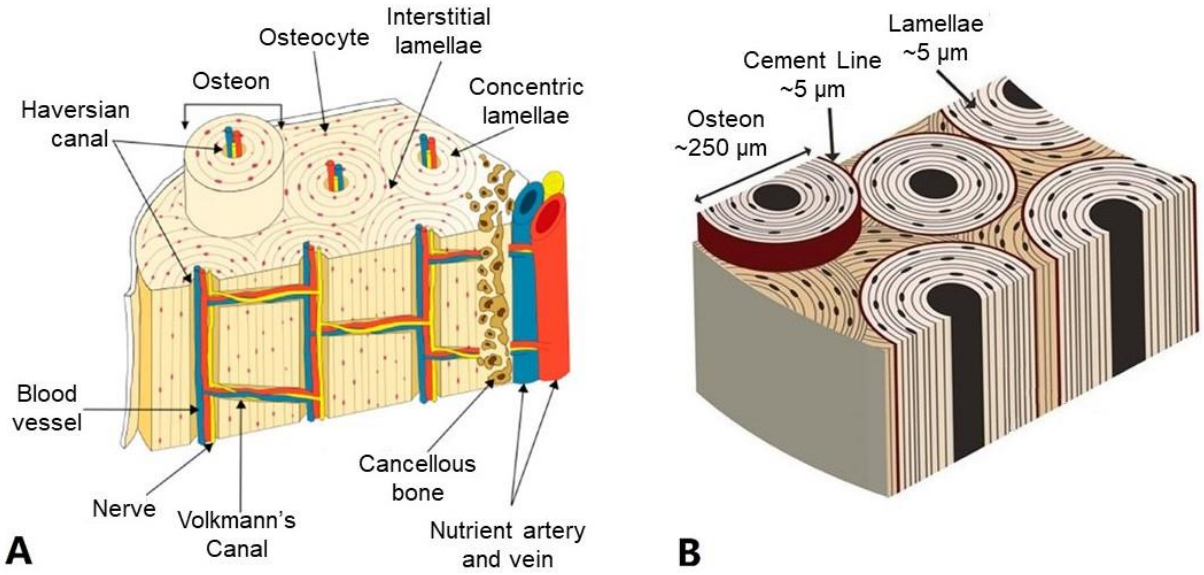

Figure 2. Bone microstructure. (A) The schematic shows the bone microstructure: osteons, concentrically arranged lamella, osteocytes, Haversian canal where blood vessels and nerves pass [40]. (B) Length-scale of bone [41] shows that the diameter of osteons ranges from 170 µm to 250 µm [35] and the thickness of cement line is less than 5 µm [36] while the lamellae, which surround vascular channel of osteons concentrically, is 2-9 µm thick [37].

Cortical bone has a higher torsional mineral resistance but a lower turnover rate than cancellous bone and can release mineral in response to deficiency [42]. On the contrary, trabecular bone has less density, more elasticity, more active turnover rate, and higher resistance to compression [42]. The rods and plates of trabecular bone align in a pattern that can provide mechanical support, maintain skeletal strength and integrity [43]. Since there is a large surface exposed to bone marrow and blood flow, trabecular bone turnover is higher than cortical bone turnover [5].

2.1.3 Bone cells

There are three types of bone cells that are responsible for bone growing and shaping including osteoblasts, osteoclasts, and osteocytes. Besides, adipocytes in bone marrow are also vital to bone remodelling and energy metabolism.

Osteocytes, which are located in lacunae, are embedded within the bone and make up more than ninety percent of all bone cells [44]. Via long dendritic processes, the osteocyte connects not only with other osteocytes but also with bone lining cells and marrow cells through the canalicular network which can also facilitate nutrition and exchange waste [45]. These functions provided by lacuna-canalicular network are essential to osteocyte viability while osteocyte network play an important role in mechnosensation and mechanotransduction [46, 47]. The viability of mechanosensitive osteocytes is a prerequisite in orchestrating bone remodelling and is critical to maintain the physiological repair procedure of bone which prevents microcracks in order to avoid succeeding fractures [46, 48, 49]. However, osteocyte viability decreases with aging through diminished canalicular network within osteons and reduced rooting and connections with the surrounding bone tissue which affects nutrition and mechanosensitivity of osteocytes and thus increases bone fragility [50]. Besides mechanosensation, the osteocyte is also responsible for regulating bone mineralization together with phosphate and calcium homeostasis [51].

Osteoblasts, which differentiate from osteogenic cells, participate in the ossification during bone turnover. Once osteoblasts are activated, rapid osteoid synthesis will be fulfilled by large Golgi apparatus and the endoplasmic reticulum of the cells [52]. In the process of osteogenesis, osteoblasts synthesize and secrete type I collagen matrix and lay down osteoid before trapping itself into mineralized bone matrix to transform into osteocytes [44]. After ossification, some of the osteoblasts become lining cells while others differentiate to osteocytes or undergo apoptosis [53].

Bone-resorbing cells, namely osteoclasts, are formed by the fusion of cells that derived from the monocyte/macrophage lineage. When osteoclast precursor cells are recruited and activated, lining cells separate from bone surface and leave the bone surface to be exposed [54]. Then preosteoclasts bind to the bone matrix and form sealing zones which isolate bone-resorbing compartments from surrounding bone [42]. The multinucleated osteoclast can dissolve mineral and digest the bone matrix by secreting hydrochloric acid and proteolytic enzymes such as cathepsin K [55, 56].

In addition to cells for bone formation and resorption, bone marrow adipocytes also play an important role in the regulation of bone remodelling and energy metabolism [57]. In normal environment, marrow adipocyte expansion reconciles with bone formation and serves as energy supporters and a source of paracrine factors to support bone formation. Nevertheless, under pathological conditions such as

physiological changes (aging and menopause), hormonal disorders, and nutritional scarcity, marrow adipose expansion occurs at the expense of osteoblast differentiation, meaning that bone marrow stem cells differentiate into adipocytes rather than osteoblasts in order to save energy [57, 58].

2.1.4 Bone turnover mechanism

Bone formation processes are divided into: intramembranous bone formation and endochondral bone formation. Intramembranous bone formation directly forms the bone which mainly takes place in flat bones such as the skull vault while the endochondral bone formation forms the majority of axial and appendicular skeleton [42]. Coordinated activities of bone formation and resorption provide mechanisms for bone turnover, which include bone modelling and remodelling. Bone modelling forms new bone and adapts structures to loading in order to maintain bone strength during growth while bone remodelling replaces old bone to repair damage [59, 60]. While bone modelling modifies bone structure such as size and shape, bone remodelling affects material properties which include collagen content, maturity, and cross-linking [60, 61]. The formation and resorption of bone modelling are uncoupled, that means the new bone is formed at one anatomical site while the old bone is removed from another [42]. However, in bone remodelling, a volume of bone resorption is followed by a comparable volume of bone deposition [60]. Bone modelling mainly takes place during growth and is influenced by mechanical loading and responsible for cortical expansion through bone formation and resorption at different skeletal sites [62]. While bone surface remodelling is common during growth, development, and in adulthood [61]. Bone remodelling takes place within a basic multicellular unit and predominantly on endo-cortical, intra-cortical, trabecular surface and less on periosteal surface [63].

Biochemical markers can be used as non-invasive assessment of bone turnover. Serum alkaline phosphatase, osteocalcin, and type I collagen extension peptides are bone formation markers while urinary calcium and hydroxyproline, and plasma tartrate-resistant acid phosphatase activity are regarded as bone resorption markers [64]. Among these, serum osteocalcin is a sensitive marker for the evaluation of vertebrae osteoporosis of female patients [64].

Bone remodelling balance can be influenced by age and diseases. Elevated bone turnover may have adverse effects on bone density and fracture risk in elderly women [65]. With age, the deposition of new bone is less than resorption of old bone which may lead to imbalance of bone remodelling and cause osteopenia or even osteoporosis [1]. Bone resorption with unfollowed bone formation can also be seen in states of mechanically unloading observed for example in patients at bed rest [66]. Other metabolic bone diseases may affect bone remodelling for example in diabetes patients, where among other bone macro and microstructure are affected by reduced cortical bone thickness and more widely spaced trabecular bone [67].

2.2 Diabetes Mellitus

Diabetes mellitus (DM), which affects over 415 million individuals worldwide [68], is a metabolic disease characterized by hyperglycemia as a result of insulin deficiency or insulin resistance [69, 70]. Due to different defects in mechanism of insulin action, DM can be classified into type 1 diabetes mellitus (T1DM), type 2 diabetes mellitus (T2DM), gestational diabetes mellitus and specific types of diabetes mellitus such as genetic defects [71, 72]. T1DM is resulting from insulin secretion deficiency while T2DM is characterized by insulin resistance.

T1DM is a chronic autoimmune disease with absolute insulin deficiency caused by destruction of the pancreatic ß-cells. It is usually diagnosed at young age and accounts for 5-10 percent of all diagnosed cases of diabetes mellitus [73]. Patients with T1DM are affected by multiple complications such as nerve defects, heart diseases, and microvascular lesions (including retinopathy and nephropathy). Increased fracture risk is also one of the complications which lays a burden on diabetic patients. However, the detailed mechanism of such a high fracture risk is still not well known. Possible reasons and the hypothesis of the caution of high fracture risk in T1DM patients are shown in Figure 3.

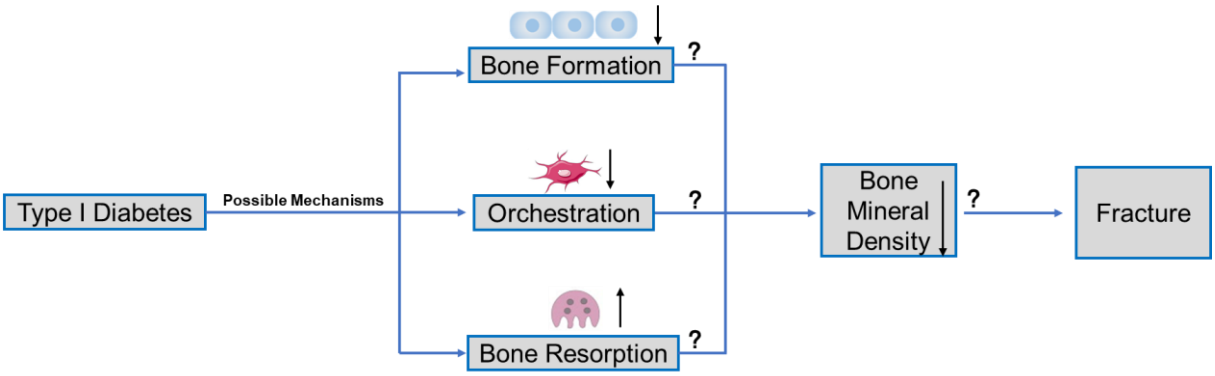

Figure 3. Possible Mechanisms of high fracture risk in T1DM patients. T1DM might increase bone resorption by osteoclast and reduce bone formation by osteoblast. Meanwhile, T1DM might reduce osteocyte number and viability by increasing osteocyte apoptosis which might in turn influence orchestration. Thus, BMD might decrease, which leads to bone fracture.

It was reported that T1DM patients have a significantly higher fracture risk and worse fracture outcome than normoglycemic individuals [74]. A meta-analysis showed that men and women with T1DM had double and quadruple higher risk for any fractures compared to subjects without diabetes respectively [75]. Among different types bone fracture sites of T1DM, vertebrae and hip are the most vulnerable skeletal sites suffering from fractures and are therefore most studied. One study showed that, postmenopausal women with T1DM had a 12 times higher incidence rate of hip fracture than those without T1DM [76]. A nurse study found that incidence of hip fracture is six-fold higher in T1DM patients than in the nondiabetic population [77]. Furthermore, the ratio of asymptomatic vertebral fracture is elevated in T1DM patients compared to non-diabetic individuals [78]. However, BMD was reported to be modestly lower at femoral neck and lumbar spine in T1DM patients compared to non-diabetic individuals in a meta-analysis and review [79]. In this research, the author mentioned that BMD is limited to explain the increased risk of fracture and underlines the importance of bone quality studies which might reveal the pathophysiology of bone fragility in T1DM patients. It is due to limited research on bone microstructure and analysis of cortical and trabecular bone in T1DM, that the mechanism of bone remodelling in T1DM is still unknown. Only few studies focused on clarifying whether the increased risk in T1DM is attributed to reduced bone mass or declined bone quality. There are no guidelines established yet for screening and preventing fracture risk in T1DM patients. In

conclusion, understanding the bone structure and underlying mechanisms in patients with T1DM may improve the prevention and treatment of the diabetic bone disease.

2.3 Dual-energy X-ray absorptiometry and bone mineral density

Dual-energy X-ray absorptiometry (DXA) is a commonly used non-invasive clinical tool for assessing patient's bone health status. By using high and low energy X-ray photons, two X-ray energy beams can be produced and attenuated by tissues to different extents. The low energy beam attenuates greater than high energy beams in soft tissue and bone, which produces a contrast of attenuation that can be used for the profile calculation. DXA is a powerful clinical instrument for osteoporosis diagnostics. It is composed of a scanning arm and an examination table (Figure 4 A). The dose of X-ray is very small and safe for children and patients. It can be used in different regions of the body such as the spine, hip, and forearm.

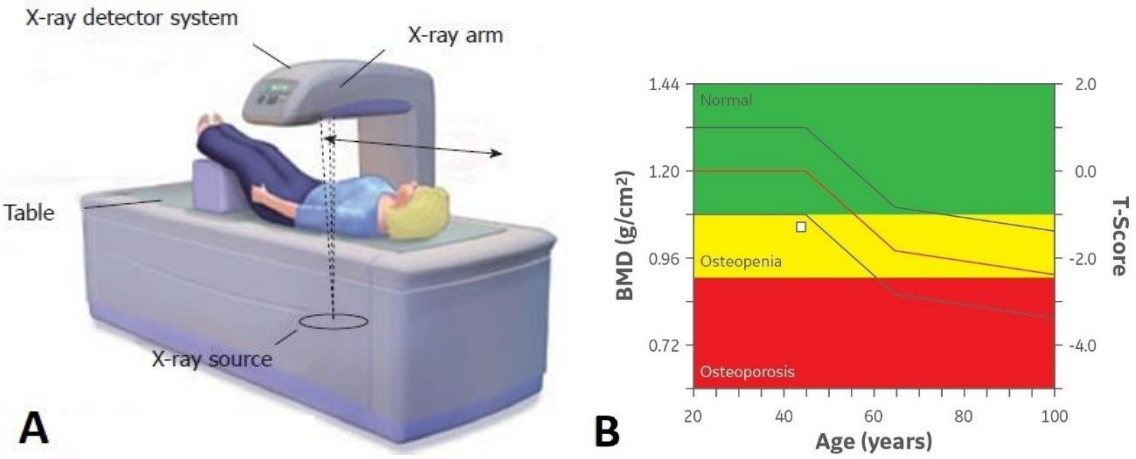

Figure 4. DXA and BMD. (A) Schematic of DXA machine shows that there is a scanning X-ray arm and an examination table for the patients. The X-ray source is under the examination table and moves together with the X-ray arm which includes a detection system [80]. (B) A graphic curve of BMD and T-score values normalized for age. The green area of the panel stands for normal T-score value (≥-1.0 SD); The yellow area indicates osteopenia (-2.5 SD<T-score<-1.0 SD) and the red part represents osteoporosis (T-score≤-2.5 SD) [80]. DXA: Dual-energy X-ray absorptiometry; BMD: Bone mineral density.

Bone mineral density (BMD) is the amount of bone mineral mass per volume of bone tissue. It accounts for up to 70% of the bone strength [81]. BMD together with

bone mineral content can be measured by DXA. Due to the strong relationship between mechanical strength and BMD or between fracture risk and BMD, DXA is considered as a 'gold standard' in osteoporosis diagnosis [82-84]. With low exposure of radiation, convenient operation, and high precision and accuracy, BMD measured by DXA is widely used for fracture risk assessment [85-87]. With BMD values, T- score and Z-score can be calculated. The T-score is based on the standard deviation of the mean BMD value of healthy young gender-matched adults while the Z-score compares BMD to the age-matched reference population [88]. A T-score above -1 SD is regarded as healthy bone, and a T-score between -1.0 SD and -2.5 SD is diagnosed as osteopenia while less than -2.5 SD represents osteoporosis (Figure 4 B). Thus, BMD analysis is an important clinical method for early identification of individuals with low bone mass and high fracture risk.

2.4 Purpose of this study

The fracture risk in T1DM patients is higher than in nondiabetic individuals. However, high fracture risk cannot be explained by normal or reduced BMD and bone mass. Until now, bone quality at the tissue-level as well as bone turnover mechanisms of T1DM bone are hardly studied. Clinical detection and treatment methods are limited due to the unknown mechanisms induced by T1DM. Thus, further studies of understanding bone turnover in T1DM are important for the prevention and treatment of vertebral fractures.

This study aims to apply DXA to measure BMD of 11^{th} thoracic - 1^{st} lumbar vertebrae and to perform histomorphometry of femoral cortical bone in T1DM and age-matched Control group to define differences of bone microstructure between individuals with and without T1DM in order to investigate how T1DM influences bone.

2.5 Hypothesis

This study focused on analysing BMD and histomorphometry parameters of T1DM and Control samples. Prior to our analysis, we hypothesized the following:

(1) BMD value of the 11th thoracic - 1st lumbar vertebrae of individuals diagnosed with T1DM present with lower BMD than age-matched healthy individuals.

(2) Bone cellular activity in T1DM is higher than non-diabetic individuals in terms of osteoclast related bone resorption in femoral mid-diaphysis.

(3) The combination of BMD and bone remodelling parameters might explain high fracture risk of T1DM patients better than BMD alone.

3. Material and methods

3.1 Sample collection

Samples collected from individuals with T1DM and age-matched healthy controls were categorized as T1DM group and Control group based on medical history. Twenty-eight vertebrae segments (19 Control and 9 T1DM, 47.11±4.98 and 48.67±6.5 years) together with fourteen femur mid-diaphysis (7 Control and 7 T1DM, 47.29±5.12 and 48±7.68 years) were collected during autopsy. All samples were supplied by the Department of Forensic Medicine at the Medical University Centre Hamburg-Eppendorf (ethic approval present). Vertebral segments were kept in medical gauze soaked with phosphate-buffered saline (PBS) and stored in the freezer at -20℃ for further research. Soft tissue, which includes muscles and ligaments, attached to each vertebra was removed before performing DXA measurements. Femur mid-diaphysis was firstly fixed in 4% paraformaldehyde for one week, and then transferred into 1 x PBS for storage.

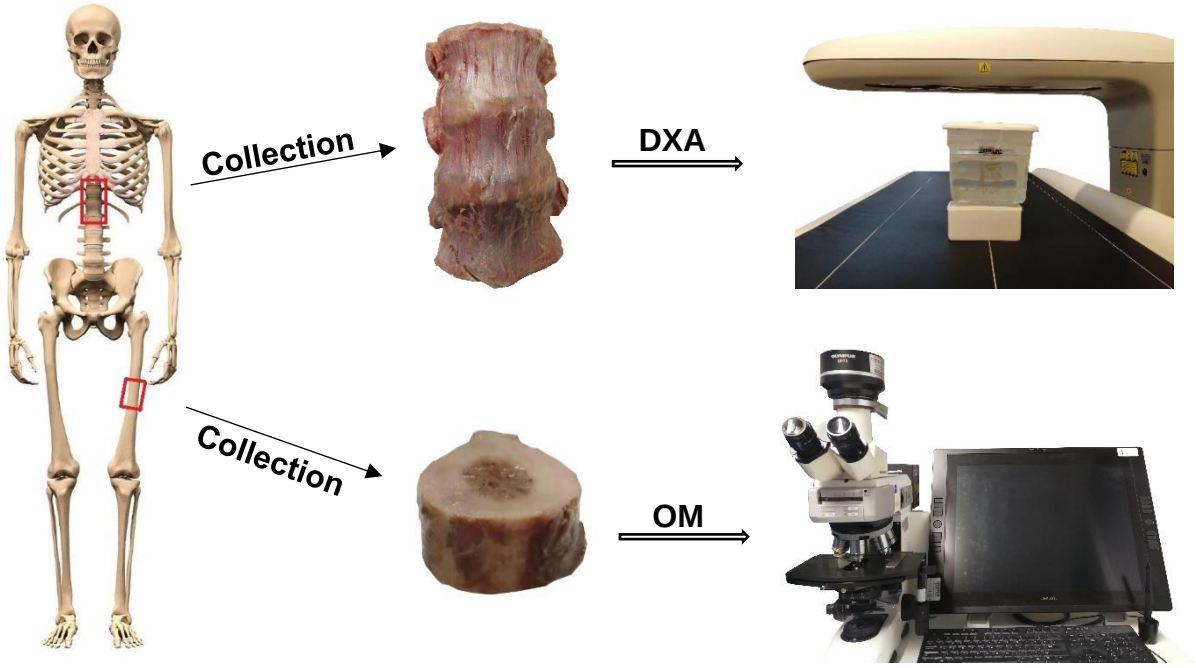

Figure 5. During autopsy 11th thoracic - 1st lumbar vertebrae were collected as well as cross-sections of femoral mid-diaphysis. Vertebrae were scanned with DXA while femoral mid-diaphysis were prepared for histomorphometry analysis with OsteoMeasure. (DXA: dual energy X-ray absorptiometry; OM: OsteoMeasure. Skeleton picture is from [89])

3.2 DXA measurement

After removal of soft tissue, a water phantom was placed on top to mimic an *in vivo* environment by simulating missing soft tissue. In this experiment, Lunar iDXA (GE Healthcare, Madison, Wisconsin, USA) was used to measure BMD of vertebra segment.

Vertebrae were placed into a plastic bag which was filled with 0.9% NaCl solution and fixed with sponges in the middle of the plastic box soaked with water in order to avoid air bubbles. After adjustment of the measurement position by the X-ray arm, the plastic box was positioned on the examination table (Figure 6 C). Anterior-posterior (AP) and lateral vertebrae positions were scanned with the DXA machine. Following the scan procedure, an image was generated to define the Region of Interest (ROI) as shown in figure 6 A and B. Finally, T-score and Z-score were calculated automatically by Lunar iDXA encore software (Version 16, GE Healthcare Madison, USA).

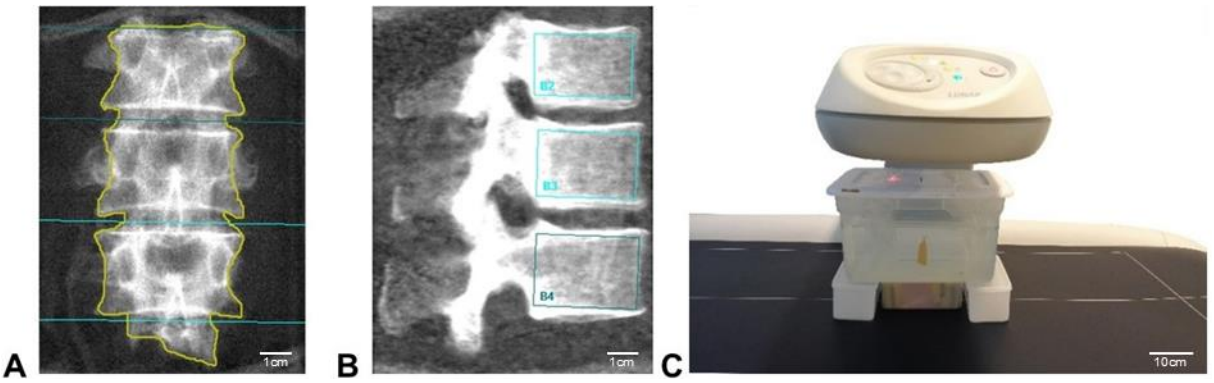

Figure 6. DXA measurement. (A) Anterior posterior direction of vertebrae during measurement shows a clear outline of 11th thoracic - 1st lumbar vertebrae segment. Yellow border is the ROI of DXA measurement. (B) Lateral position of vertebrae in DXA measurement shows high density in superior articular process, transvers process, lamina, and inferior articular facet. ROI of lateral scan can be seen in the schematic above. (C) Water phantom mimics *in vivo* BMD measurement on DXA machine table.

3.3 Embedding, grinding and staining

Femoral mid-diaphysis samples were sawed (Diamond Band Saw, Exakt, Norderstedt, Germany) into 4 mm-thick cross-sections with a diamond belt saw. After performing X-ray (Faxitron LX-60, Lincolnshire, England), the anterior part of the femoral cross- section was extracted (Figure 7 A). Next, the anterior quadrant was

dehydrated automatically in increasing concentration of 80%, 96%, and 100% ethanol overnight (Autotechnicon, Enno Vieth, Wiesmoor, Germany). Samples were infiltrated in Infiltration I for 24 hours and Infiltration II for 5 days (see appendix) at 4℃. Following methylmethacrylat infiltration, the bone samples were placed into small glass jars which were filled with the embedding solution (shown in appendix I). The jars were transferred into the refrigerator at 4℃ overnight for polymerization in order to get polymerized methylmethacrylat (PMMA) blocks.

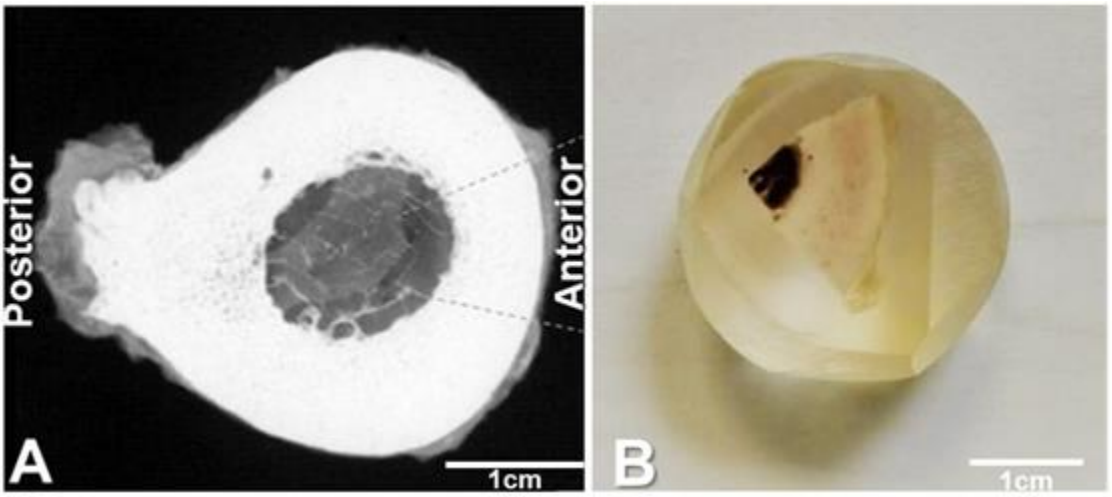

Figure 7. (A) X-ray image of a cross section of femur mid-diaphysis. Anterior part was obtained for later histomorphometry analysis. (B) PMMA block with embedded anterior quadrant of femoral mid-diaphyseal bone.

All PMMA blocks (Figure 7 B) were used for cutting thin sections and preparing ground sections. Following cutting into 4 µm sections, the sections were transferred 3 times into 2-Methoxyethyl-Acetat to remove PMMA from the tissue for 5 minutes each. For rehydration the sections were transferred into decreasing ethanol series of 100%, 96%, 80%, 70%, and 50% ethanol for 2 minutes each. After rinsing the sections in distilled water for 3-5 minutes, the sections were stained with 1% Toluidine Blue liquid (pH 4.5) for 30 minutes. For dehydration samples were transferred into 50%, 70%, 80%, 96%, and 100% ethanol for 2 minutes each and 3 times into Xylol for 5 minutes each. Finally, the sections were covered with coverslip. For the ground section, the embedded anterior quadrants were ground until co-parallel and the surface was polished with an automatic grinding machine (D-2000, Exakt, Norderstedt, Germany) to diminish surface roughness. Then Technovit 7210 (Kulzer GmbH, Wehrheim,

Germany) was applied for sample gluing on a transparent plastic slide. Samples were put under ultraviolet light for 30 minutes and then positioned in a slice holder of a diamond band saw (300, Exakt, Norderstedt, Germany) to cut the sample. Samples were ground again in the automatic grinding machine until the thickness of the section reached up to 80 µm. After polishing, samples were transferred into 10% hydrogen peroxide (H_2O_2) for 10 minutes and then stained with Toluidine blue (pH 4.5) for 30 minutes.

3.4 Histomorphometry analysis

3.4.1 Thin section

Among the 14 femoral mid-diaphyseal sections, we analysed 5 Control and 5 T1DM femoral thin sections. These femoral mid-diaphyseal cross-sections were scanned under the microscope (Olympus, Tokyo, Japan) to obtain an overview image. The total area of bone ROI was selected to be in the central of endo-cortical bone (Figure 8 A). With OsteoMeasure (OsteoMetrics, Atlanta, GA, USA) and the histomorphometry parameters presented in Table 1 were evaluated on the cortical bone section. The total analysed ROI of endo-cortical bone was 4 mm^2. Disconnected trabecular bone was excluded during the measurement.

Meanwhile, bone marrow adipocytes close to endo-cortical region were also measured (Figure 8 B). Since bone marrow was not preserved and could not be analysed in one sample per group, 8 anterior quadrants of femoral mid-diaphysis (4 Control and 4 T1DM) were analysed regarding adipose tissue. The ROI of adipose tissue is located in the bone marrow near endo-cortical border with an area of 1.25 mm^2. Incomplete adipocytes, presented at the border which were not completely in the ROI, were excluded during the measurement. Adipocyte number, perimeter, diameter, and area were automatically calculated by the software OsteoMeasure.

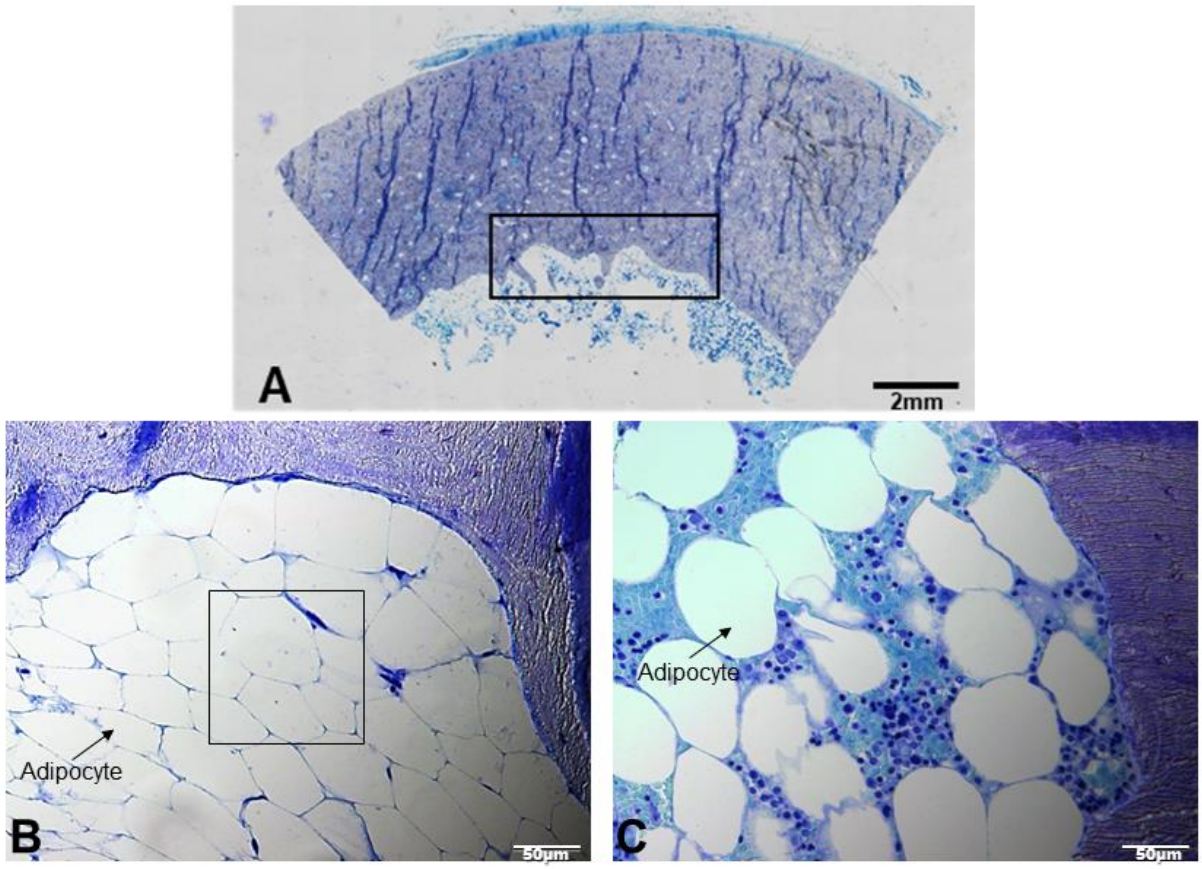

Figure 8. (A) Overview of Toluidine Blue staining of femoral anterior quadrant. ROI is shown by the black rectangle. (B) and (C) Adipose tissue and adipocytes. The square ROI is shown in the image (Scale bar: 50µm).

Table 1. Parameters of bone histomorphometry measured with OsteoMeasure

Parameters	**Abbreviation**	**Units**
Number of osteocytes per bone area	N.Ot/B.Ar	#/mm^2
Number of empty lacunae per bone area	N.EmLa/B.Ar	#/mm^2
Number of osteocytes per total number of lacunae	N.Ot/Tt.No	%
Bone surface per bone volume	BS/BV	1/mm
Bone area per total area	B.Ar/T.Ar	%
Eroded surface per bone surface	ES/BS	%
Osteoclast surface per bone surface	Oc.S/BS	%
Number of osteoclasts per bone surface	N.Oc/BS	#/mm
Osteoblast surface per bone surface	Ob.S/BS	%
Number of osteoblasts per bone surface	N.Ob/BS	#/mm
Osteoid volume per bone volume	OV/BV	%

Osteoid surface per bone surface	OS/BS	%
Osteoid thickness	O.Th	mm
Adipocyte area per total marrow area	Ad.Ar/Tt.Ar	%
Number of adipocytes per total marrow area	N.Ad/Tt.Ar	#/mm
Adipocyte diameter	Ad.D	μm
Adipocyte perimeter per number of adipocytes	Ad.P/N.Ad	mm

3.4.2 Ground section

The anterior quadrant of femoral mid-diaphyseal cross-sections embedded in PMMA blocks of 14 samples (7 Control and 7 T1DM) were used to make ground sections. The whole cross-section was horizontally divided into three equal parts: Peri-cortical, intra-cortical, and endo-cortical using the method of Jasmine and Heilmeier (Figure 9 A) [90, 91]. Image J was used to do the segmentation of the ground section (Figure 9 B).

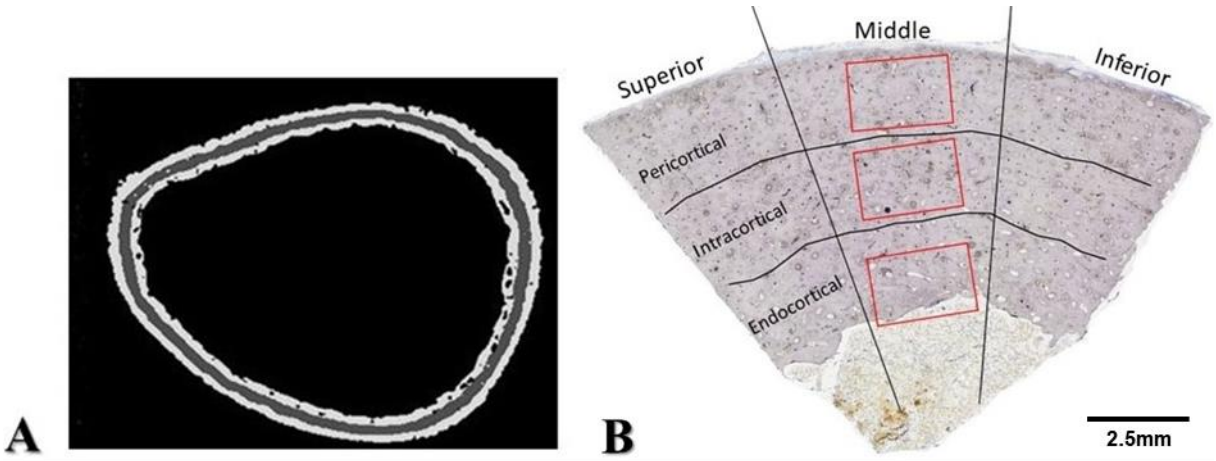

Figure 9. Segmentation of bone. (A) The cross-section of distal tibia scanned from HR-pQCT was divided equally into peri-, intra-, and endo-cortical part [91]. (B) Image J was used to separate the anterior region of femur mid-diaphyseal cortex into peri-, intra-, and endo-cortical as well as superior, middle, and inferior part. Three red rectangles show the ROI in peri-, intra-, and endo-cortical region, respectively.

The whole cross-section was longitudinally divided into superior, middle, and inferior part equally. Histomorphometry was performed with the software

OsteoMeasure. Each 4 mm^2 ROI was measured in three regions (peri-cortical, intra-cortical, endo-cortical) respectively and 12 mm^2 was measured in total. The ROI was located at the middle region of the whole section and is shown in Figure 10 B. The ROI in endo-cortical region covered the endosteal border while in peri-cortical region ROI was close to but not across the periosteal border. The ROI in all 3 regions is measured with a microscope (Olympus, Tokyo, Japan) with a 20 x objective.

3.5 Statistical analysis

Statistical analysis was performed using SPSS (Version 22, IBM, Armonk, NY, USA). At the beginning, normality of data was tested with Shapiro-Wilk test and homogeneity of variances was determined with Levene's test. Student t test was used to analyse normally distributed data between Control and T1DM group while Mann-Whitney U test was used to compare not normally distributed data. In each group, One-Way ANOVA (Bonferroni and Games-Howell) and Friedman test were chosen to compare normally and not normally distributed data respectively. Wilcoxon test (two related samples test) was used to compare the data between thin section and ground section. Data was presented as mean ± standard deviation (SD) and a p value of less than 0.05 was regarded as statistically significant. Interquartile range (IQR) was calculated and outliers (values less than Q1-1.5*IQR or large than Q3+1.5*IQR) in each group were excluded from the original data.

4 Results

4.1 DXA results of bone mineral density

BMD results are presented in Figure 10. The AP and lateral BMD of 11th and 12th thoracic vertebrae and 1st lumbar vertebra together with 1st lumbar T-score and Z-score are obtained from the DXA measurement. Due to the damage of some vertebrae segments, we are only able to analyse 11th thoracic vertebrae of 22 samples (15 Control and 7 T1DM), 12th thoracic vertebrae of 25 samples (17 Control and 8 T1DM), and 1st lumbar vertebrae BMD, T-score, and Z-score of 25 samples (16 Control and 9 T1DM).

BMD of 11th thoracic vertebra in AP direction in T1DM and Control groups are 0.967±0.122 g/cm^2 and 0.984±0.201 g/cm^2 respectively (p=0.841). While AP BMD of 12th thoracic vertebra in T1DM and Control groups are 0.898±0.134 g/cm^2 and 0.926±0.200 g/cm^2 respectively (p=0.726). Both AP BMD values of 11th and 12th thoracic vertebrae in Control group are similar comparing to that in T1DM group (without statistical difference). Furthermore, AP BMD of 1st lumbar vertebra in Control (1.012±0.209 g/cm^2) is the same as that in T1DM (1.025±0.110 g/cm^2, p= 0.856).

BMD of 11th thoracic vertebra in lateral position presents with 0.629±0.148 g/cm^2 and 0.638±0.126 g/cm^2 in T1DM and Control groups respectively (p=0.680) and 0.599±0.164 g/cm^2 and 0.657±0.163 g/cm^2 in 12th thoracic vertebra in T1DM vs. Control respectively (p=0.413). For 1st lumbar vertebra, the lateral BMD is 0.599±0.158 g/cm^2 in T1DM and 0.663±0.156 g/cm^2 in Control (p=0.352). Lateral BMD values of 11th thoracic - 1st lumbar vertebrae are all similar in Control group compared to T1DM group.

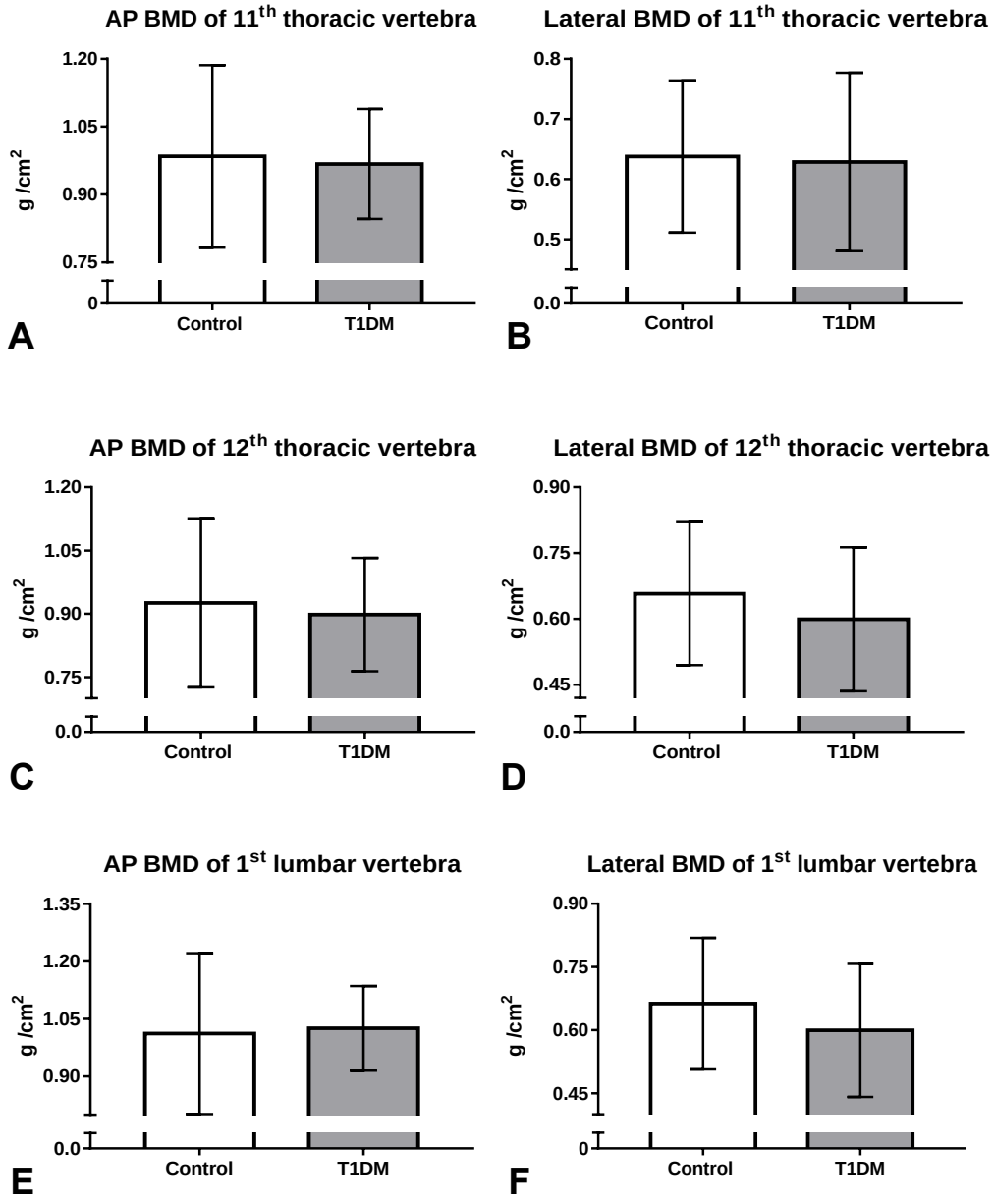

Figure 10. AP and Lateral BMD of 11th thoracic - 1st lumbar vertebrae in T1DM and Control groups. (A) AP BMD value of 11th thoracic vertebrae in T1DM is similar to that in Control group ($p > 0.05$). (B) Lateral BMD value of 11th thoracic vertebrae in T1DM is the same as that in Control group ($p > 0.05$). (C) AP BMD value of 12th thoracic vertebrae in T1DM is similar to that in Control group ($p > 0.05$). (D) Lateral BMD value of 12th thoracic vertebrae in T1DM is equal to that in Control group ($p > 0.05$). (E) and (F) show 1st lumbar vertebra AP and lateral BMD in T1DM are equal to that in Control group ($p > 0.05$). T1DM: Type 1 diabetes mellitus; AP: Anterior-Posterior; BMD: Bone mineral density.

The T-score and Z-score of 1st lumbar vertebra (Figure 11) in Control (-1.188±1.710 and -0.806±1.810, respectively) are also the same as that in T1DM (-

1.033±0.872 and -0.656±0.819, respectively), with p values 0.804 and 0.778 respectively.

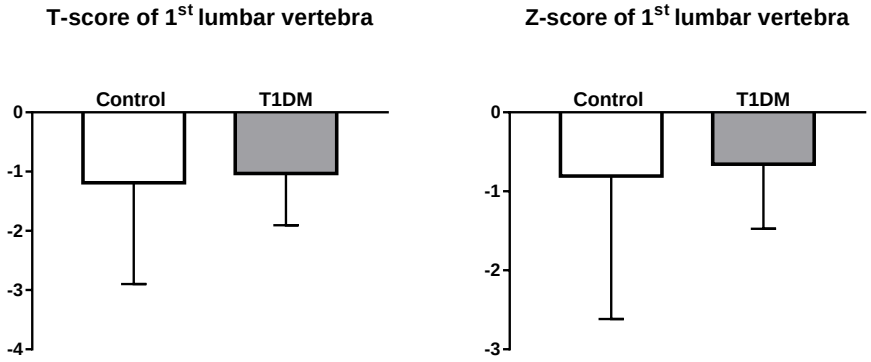

Figure 11. T-score and Z-score of 1st lumbar vertebra. The histogram shows that T-score and Z-score of 1st lumbar vertebra in AP position are similar in T1DM and Control groups.

4.2 Histomorphometry results

4.2.1 Histological section

Ten samples (5 Control and 5 T1DM) are processed to cut thin section. After staining with Toluidine Blue, the osteocytes are characterized by dark blue cell nuclei shown in Figure 12. And empty lacunae are identified by absence of cell nuclei.

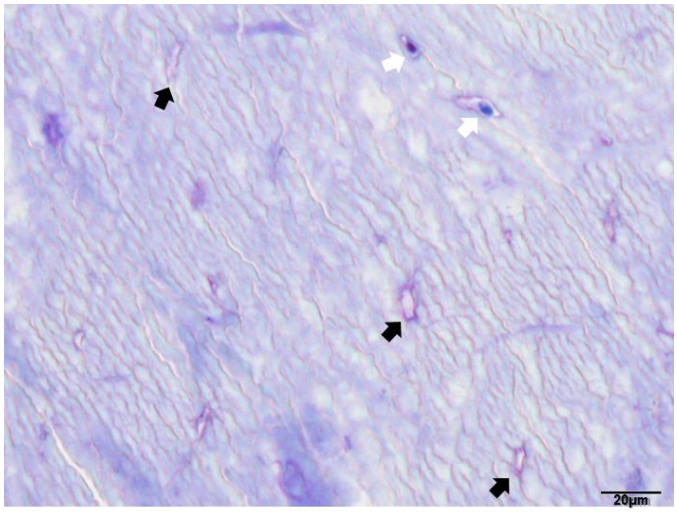

Figure 12. Osteocytes with cell nuclei are marked by white arrows and empty lacunae are labelled by black arrows (Scale bar: 20µm).

Osteoblasts are found only in one of the T1DM samples. Dark blue osteoblast lining around light blue osteoid is shown clearly in Figure 13 A. Data shows that osteoblast surface per bone surface (Ob.S/BS) is 2.267% and number of osteoblasts per bone surface (N.Ob/BS) is 1.390 #/mm. Meanwhile, osteoid volume per bone volume (OV/BV), osteoid surface per bone surface (OS/BS), and osteoid thickness (O.Th) are 0.328%, 3.458%, and 1.390 µm respectively. However, no osteoblast is found in each of the femoral anterior quadrant in Control group. Osteoclasts are only found in another T1DM sample (Figure 13 B). And data shows osteoclast surface per bone surface (Oc.S/BS) is 0.101% and number of osteoclasts per bone surface (N.Oc/BS) is 0.048 #/mm. The related eroded surface per bone surface (ES/BS) is 0.250%.

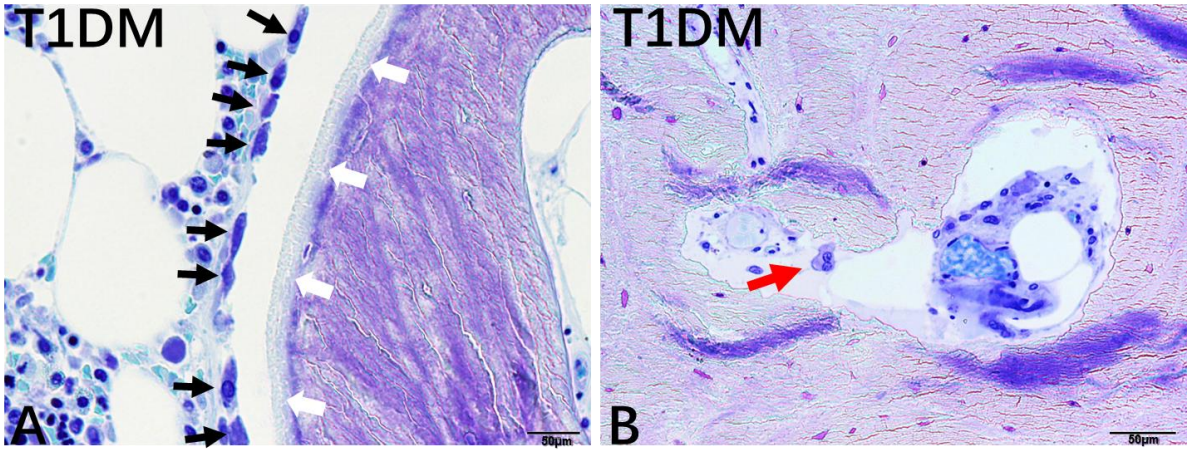

Figure 13. Osteoblast and osteoclast in Toluidine Blue stained section (Scale bar: 50µm). (A) Osteoblasts, shown by black arrows, can be seen lining around the bone on top of light blue osteoid attached to the surface of endo-cortical bone where white arrows are pointing. (B) An osteoclast is shown by a red arrow in the void area of the bone. There is also eroded surface surrounding the bottom of the osteoclast.

There is no osteoid without osteoblast (Figure 14 A) inside the ROI of Control and T1DM groups. However, eroded surface without osteoclast (Figure 14 B) is found in both Control and T1DM samples.

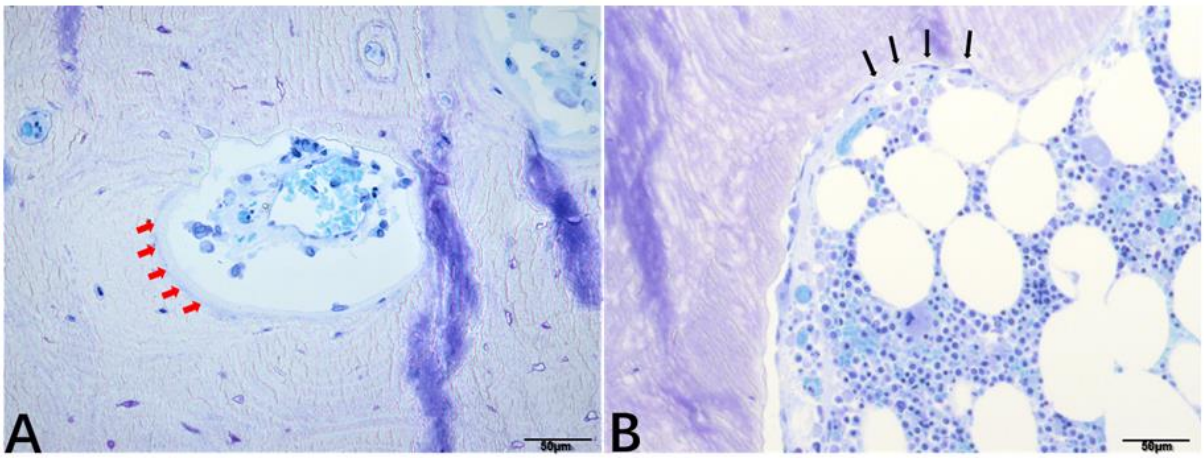

Figure 14. Osteoid and eroded surface (Scale bar: 50µm). (A) Osteoid is found outside the ROI and there is no osteoblast on the top of it (osteoid is labelled by red arrows). (B) Eroded surface can be seen in endo-cortical bone (labelled by black arrows).

Cellular activity measurement results are shown in Figure 15. As can be seen in Figure 15 A, bone surface per bone volume is similar in Control and T1DM groups (5.416±0.868/mm vs. 7.486±2.941/mm respectively, p=0.175). Bone volume per total volume (Figure 15 B) is 75.534±1.419% and 73.027±7.594% in Control and T1DM groups respectively (p=0.886). While the number of osteocytes per bone area (Figure 15 C) is 81.386±13.324 #/mm^2 in Control group and 94.213±16.262 #/mm^2 in T1DM group (p=0.251). The number of empty osteocyte lacunae per bone area (Figure 15 D) shows similar results comparing Control and T1DM groups with 80.763±25.402 #/mm^2 and 119.113±30.599 #/mm^2 respectively (p=0.175). Meanwhile, the number of living osteocytes per total number of lacunae (Figure 15 E) are comparable in Control and T1DM groups (50.988±4.642% and 44.658±9.184% respectively, p=0.251). Looking at bone resorption, the eroded surface per bone surface (Figure 15 F) presents with a lower value in the Control group compares to T1DM group (8.390±5.223 % and 17.957±3.389 % respectively, p=0.036).

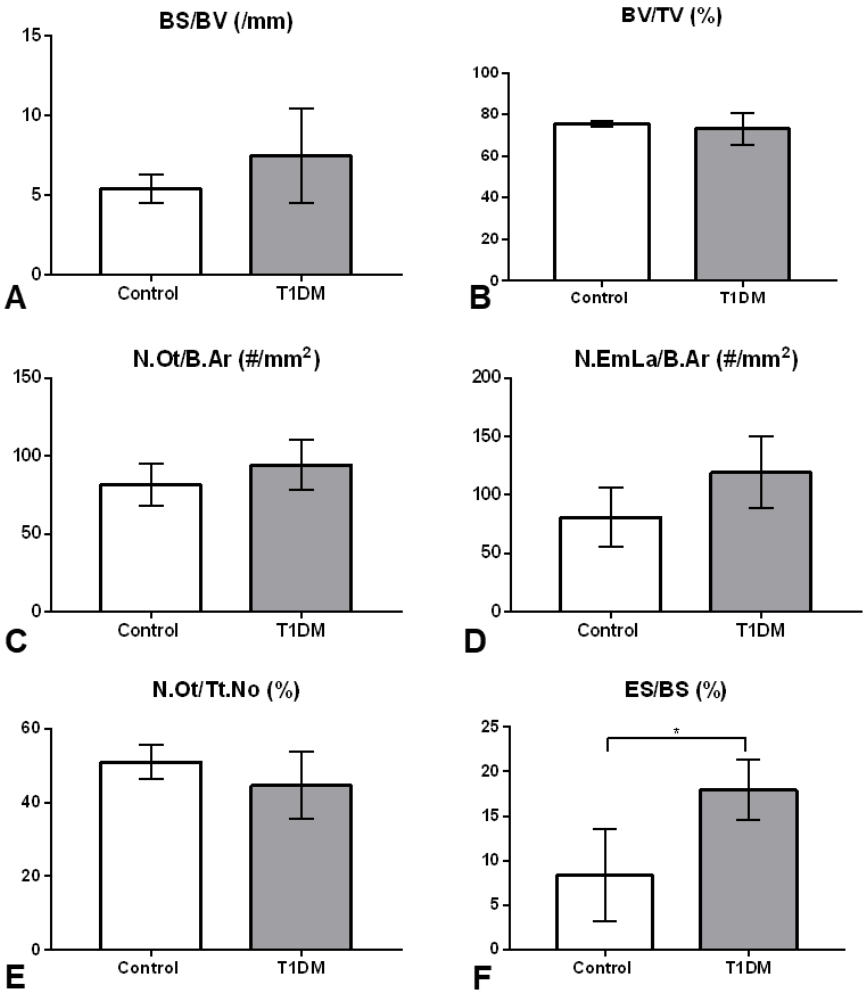

Figure 15. Bone histomorphometry results of Control and T1DM groups. (A) Bone surface per bone volume in T1DM is similar compared to Control. (B) Bone volume per total volume shows no difference between the two groups. (C) Number of osteocytes per bone area in T1DM group is the same as in Control group. (D) Number of empty lacunae per bone area is the same in T1DM and Control groups. (E) Number of osteocytes per total number of lacunae is similar in T1DM and Control groups. (F) Eroded surface per bone surface presents with a higher trend in T1DM than Control group (p=0.036).

Adipocyte diameter (Figure 16 A) is the same for both groups with 54.317±0.625 μm and 52.372±11.417 μm in Control and T1DM groups respectively (p=0.857). Single adipocyte perimeter (Figure 16 B) is 0.202±0.020 mm and 0.206±0.012 mm in Control and T1DM groups respectively (p=0.773). Number of adipocytes per bone marrow area (Figure 16 C) is measured with 224.370±63.442 #/mm^2 and 285.755±174.958 #/mm^2 (p=0.564). Adipocyte area per total marrow area (Figure 16 D) presents with 63.723±21.714% and 69.400±24.356% in Control and T1DM groups respectively (p=0.564).

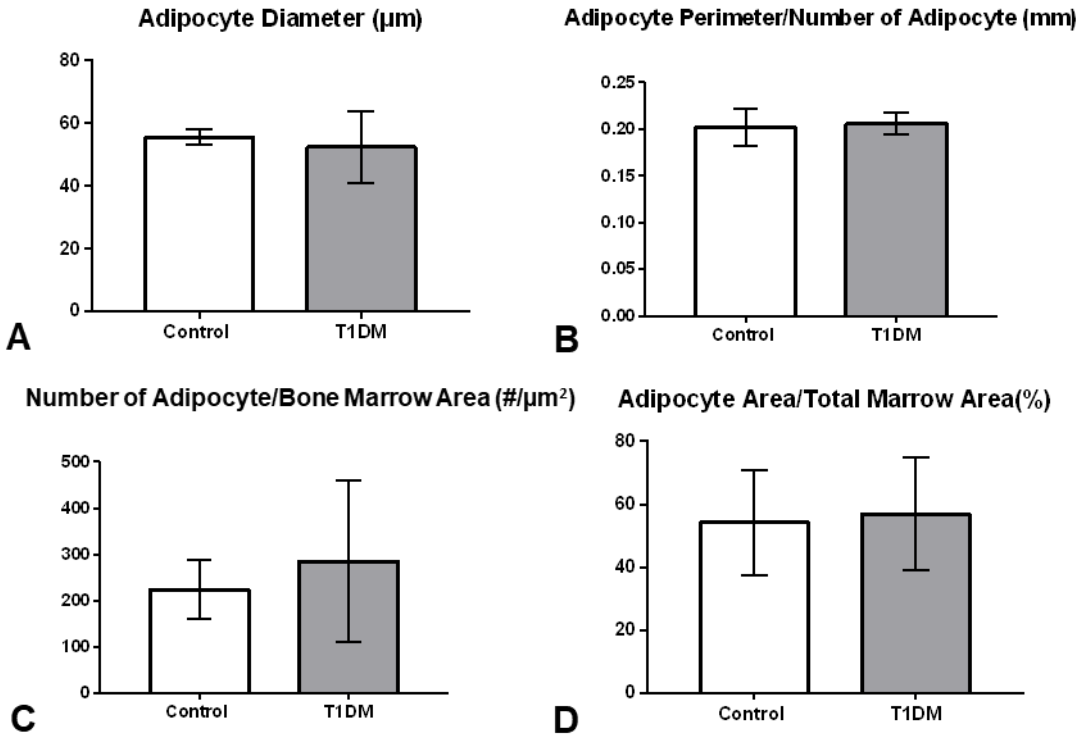

Figure 16. Bone marrow adipose tissue analysis. (A-D) Similar results are found in adipocyte diameter, perimeter, number and area between Control and T1DM groups.

4.2.2 Ground section

Due to the inevitable artifacts during the sample cutting procedure, overlapping and cracks are found in thin sections which might influence the accuracy with increasing difficulties. In order to solve this problem, ground sections are made to narrow this gap and pursue a better quality during the analysis.

In ground sections, osteoblasts are found in 2 samples of Control group in peri-cortical region while present in only 1 sample of T1DM group in endo-cortical region which is shown in Figure 17 A and B. In the peri-cortical region of these 2 Control samples, Ob.S/BS is 0.600% and 1.454% while N.Ob/BS is 0.5976 #/mm and 0.903 #/mm. Furthermore, OV/BV is 0.033% and 0.033% and OS/BS is 0.600% and 1.454% while O.Th is 6.500 µm and 4.362 µm in the peri-cortical region of the two samples. In the endo-cortical region of the T1DM sample, Ob.S/BS, N.Ob/BS, OV/BV, OS/BS, and O.Th values are 1.152%, 0.702 #/mm, 0.114%, 3.771%, and 5.092 µm respectively.

Osteoclasts are found in endo-cortical region of 1 T1DM sample (Figure 17 C and D). Oc.S/BS is 0.504% and N.Oc/BS is 0.195 #/mm. ES/BS is 0.925% in T1DM endo-cortical region. However, no osteoclast is observed in any region of the Control samples.

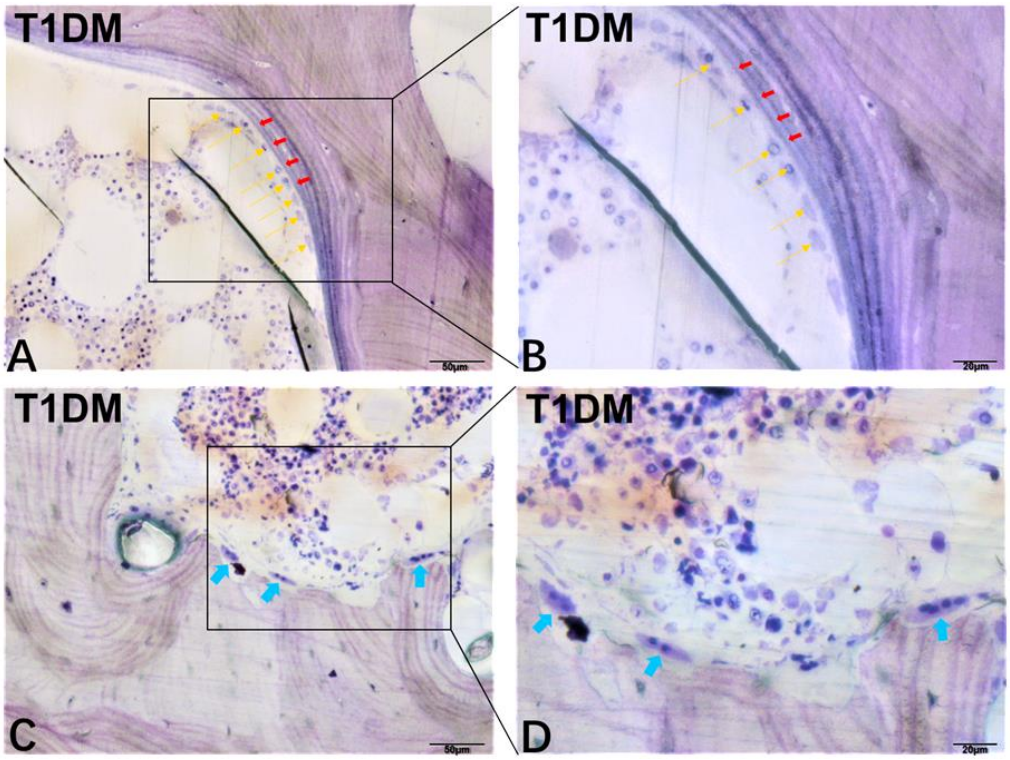

Figure 17. Images of ground section show bone formation and resorption signs in femoral cortex. (A) Several osteoblasts on top of osteoid in endo-cortical region (Scale bar: 50 μm). (B) Zoom in of osteoblasts (Scale bar: 20 μm). (C) Osteoclasts on eroded surface (Scale bar: 50 μm). (D) Zoom in of osteoclasts (Scale bar: 20 μm).

The results show that BS/BV (Figure 18 A) is higher in endo-cortical region than peri-cortical region within both Control and T1DM groups comparison (p=0.037 and p=0.002, respectively). However, BS/BV in endo-, intra-, and peri-cortical region is similar between Control and T1DM groups. On the contrary, BV/TV (Figure 18 B) is lower in endo- than peri-cortical region within Control group (p=0.004). And BV/TV is lower in endo-cortical region than intra- and peri-cortical region within T1DM group (p<0.001 respectively). BV/TV in endo-cortical region of Control group is higher than that in T1DM group (p=0.012) while no significant difference can be found in intra- or peri-cortical region between Control and T1DM groups.

N.Ot/B.Ar (Figure 18 C) is higher in endo-cortical region in Control group than T1DM group (63.874±16.208 #/mm^2 and 43.555±13.075 #/mm^2, p=0.035). However, no difference is found in intra-cortical and peri-cortical regions between Control and T1DM groups. The values are 50.149±11.267 #/mm^2 and 50.943±22.713 #/mm^2 (p=0.936) in intra-cortical region, 48.846±5.687 #/mm^2 and 59.375±22.076 #/mm^2 (p=0.262) in peri-cortical region in Control and T1DM groups respectively.

N.EmLa/B.Ar (Figure 18 D) in each region of the Control group is also the same as in T1DM group. The values are 154.468±44.690 #/mm^2 and 117.288±12.531 #/mm^2 (p=0.051) in endo-cortical region, 177.752±52.058 #/mm^2 and 143.244± 56.777 #/mm^2 (p=0.259) in intra-cortical region, 157.002 ± 45.780 #/mm^2 and 142.156 ±41.948 #/mm^2 (p=0.539) in peri-cortical region in Control and T1DM groups respectively.

N.Ot/Tt.No (Figure 18 E) in each region of Control and T1DM groups are similar. Data shows 29.725±6.589% and 31.044±6.267% (p=0.731) in endo-cortical region, 22.798±6.022% and 27.305±10.307% (p=0.337) in intra-cortical region, 22.533±3.387% and 30.285±11.273% (p=0.295) in peri-cortical region in Control and T1DM groups respectively.

ES/BS (Figure 18 F) in endo-cortical region presents with 0.652±0.830% and 1.141±1.182% in Control and T1DM groups respectively (p=0.306). However, in intra-cortical region of T1DM group, eroded surface is only observed in one sample whereas in peri- cortical region of Control group, eroded surface is found in no samples.

Osteoid thickness and perimeter are shown in Figure 18 G and H. There is no significant O.Th difference in endo- or peri-cortical region between Control and T1DM groups (p=1.000 and p=0.400 respectively). OS/BS also shows similar results in endo- or peri-cortical region between Control and T1DM groups (p=0.700 and p=1.000 respectively). However, statistical comparison cannot be made in intra-cortical region between Control and T1DM groups due to the fact that osteoid was found in only limited samples.

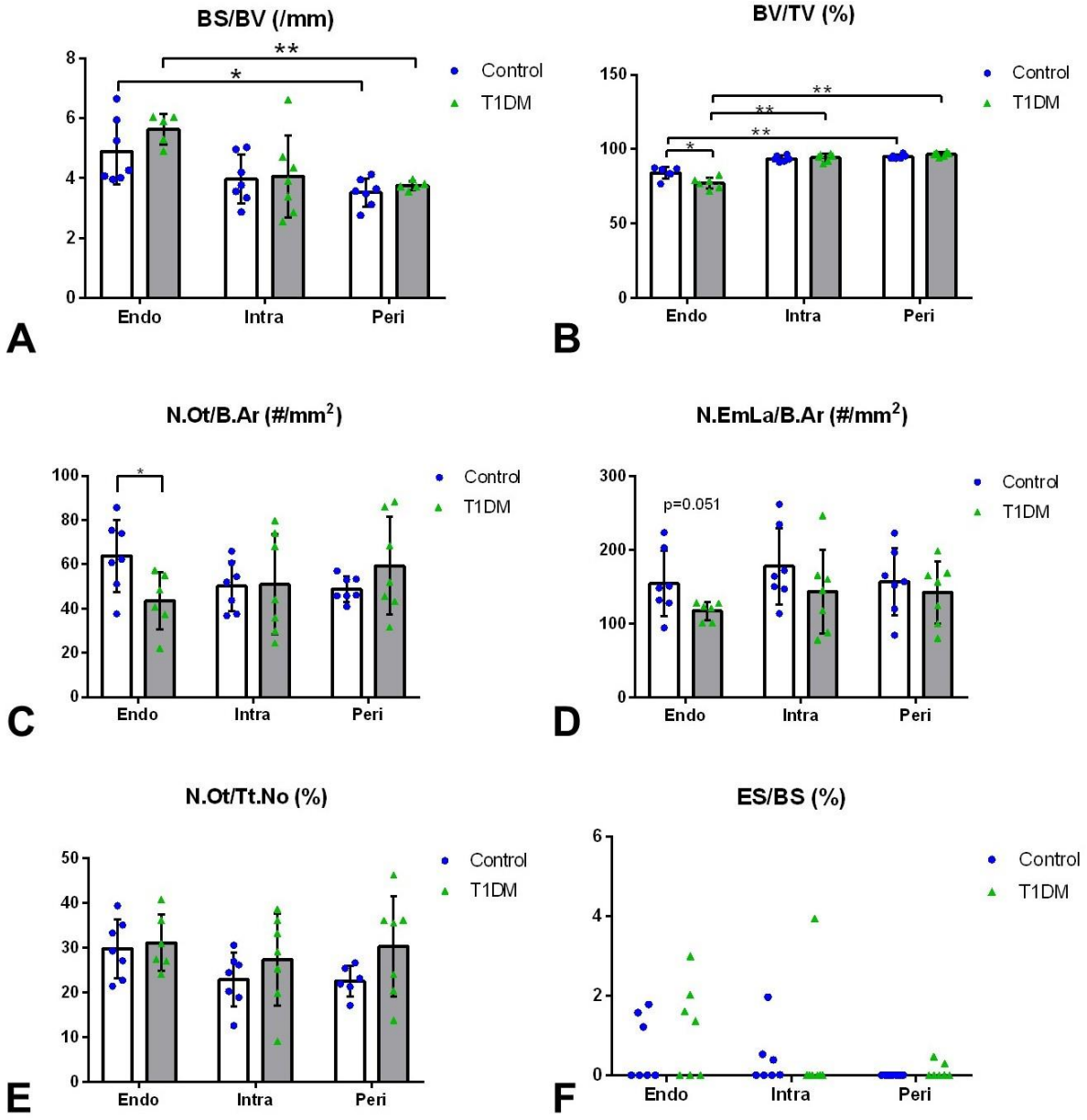

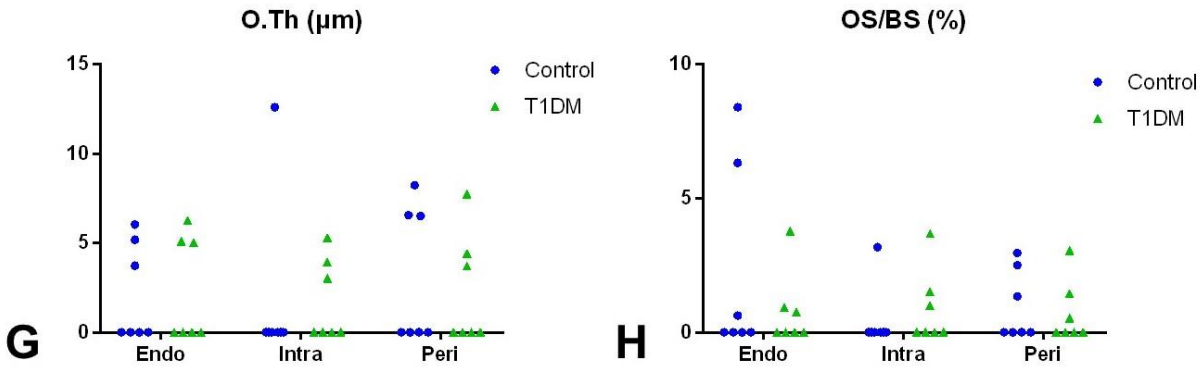

Figure 18. Bone tissue histomorphometry results. (A) Bone surface per bone volume in endo-cortical region is higher than peri-cortical region in both Control and T1DM groups. (B) Bone volume per tissue volume is lower in endo-cortical region than peri-cortical region in Control and T1DM groups. (C) Number of osteocytes in endo-cortical region is lower in T1DM than Control group. However, it is similar in intra- and peri-cortical regions in Control and T1DM groups. (D) Number of empty lacunae are similar in Control compared to T1DM group. (E) No difference is found regarding osteocyte percentage of total lacunae between Control and T1DM groups. (F) Similar eroded surface is found in endo-cortical region of Control and T1DM groups. (G) There is no difference in osteoid thickness in endo- or peri-cortical region between Control and T1DM groups. (H) Osteoid surface per bone surface is the same in the related regions of Control and T1DM groups. (*p<0.05, **p<0.005)

4.2.3 Comparison between thin and ground sections

Comparison between thin and ground sections histological data in endo-cortical regions are shown in Table 2 and Figure 19. There is no difference in BS/BV and BV/TV between thin and ground sections. However, N.Ot/B.Ar , N.Ot/Tt.No, and ES/BS are significantly higher in thin section than ground section while N.EmLa/B.Ar is lower in thin section compares to ground section.

Table 2. histological data of thin and ground sections

	Control		T1DM	
	Thin section	Ground section	Thin section	Ground section
BS/BV (/mm)	p=0.500		p=0.225	
BV/TV (%)	p=0.500		p=0.225	
N.Ot/B.Ar (#/mm^2)	p=0.043		p=0.043	

N.EmLa/B.Ar (#/mm^2)	p=0.043	p=0.893
N.Ot/Tt.No (%)	p=0.043	p=0.043
ES /BS (%)	p=0.043	p=0.043

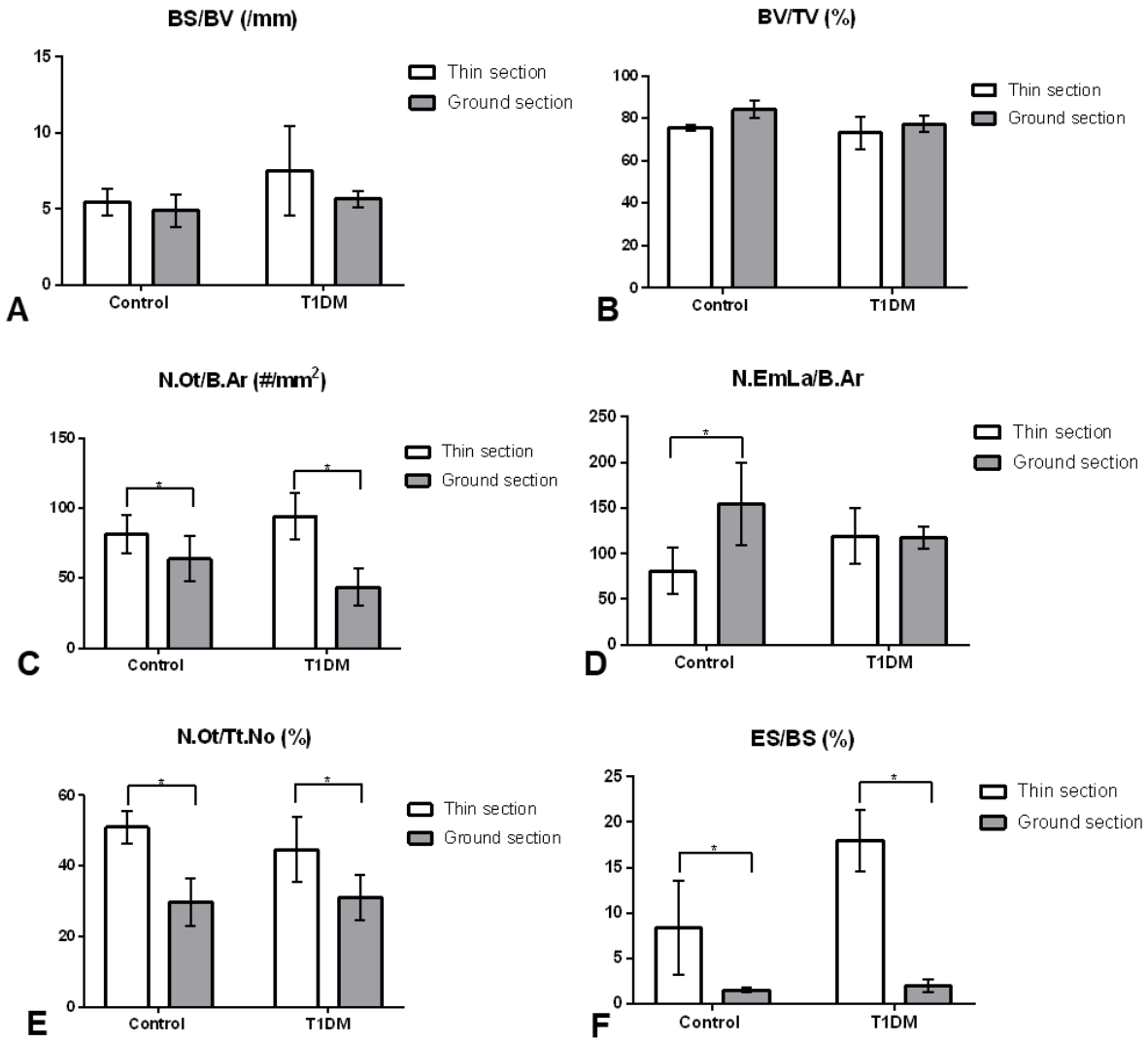

Figure 19. Comparison between thin and ground sections results. (A) Bone surface per bone volume in endo-cortical region of ground section is similar to thin section. (B) Bone volume per tissue volume in endo-cortical region of ground section is similar to thin section. (C) Number of osteocytes is higher in thin section compared to ground section in both Control and T1DM groups (p=0.043). (D) Number of empty lacunae is lower in thin section compared to ground section with regard to Control group (p=0.043), however, not in T1DM group. (E) Number of osteocytes per total number of lacunae is higher in thin section than ground section in both Control and T1DM groups (p=0.043). (F) Eroded surface in thin section is higher than ground section in both Control and T1DM groups (p=0.043).

5 Discussion

5.1 Bone mineral density and cellular activity in T1DM

This study shows that BMD values of 11th and 12th thoracic vertebrae together with 1st lumbar vertebra are all similar in both Control and T1DM groups. Statistical analysis shows that no significant difference is found between Control and T1DM groups regarding BMD value of any segment from 11th thoracic to 1st lumbar vertebrae. For histological data, eroded surface is higher in T1DM group than Control group (thin section) while osteocyte number is higher in endo-cortical region of Control group than T1DM group (ground section).

There are studies showing that BMD in T1DM patients is different from non-diabetic individuals in contrast to our BMD results. In a cross-sectional study by Neumann et al. [92], Ingberg et al. [93], and Rakic et al. [94], a slightly lower BMD value at both lumbar spine and femoral neck in male and female patients with T1DM compared to non-diabetics was reported. However, BMD of lumbar spine and femoral neck in females was higher in T1DM according to the result of Lunt et al. [95] and Leidig-Bruckner et al. [96]. Furthermore, Slade et al. [97] reported higher lumbar spine BMD in both male and female patients with T1DM compared to Control. In a meta-analysis [79], it was shown that BMD at femoral neck was modestly lower (−0.055 g/cm^2) in T1DM patients than Controls which was also confirmed in other meta-analysis of Vestergaard et al. [98] and Pan et al. [99]. This might be due to different studies adopting different measurement sites, for example lumbar vertebrae, hip, radius, or even the whole body. Furthermore, confounding factors such as age, gender, and pre- or postmenopausal status in women also influence BMD value with regard to comparison in diabetic and non-diabetic individuals.

Here we present the analysis of cellular activity in cortical bone from femoral mid-diaphysis combined with an *ex vivo* approach to link femoral histomorphometry results to vertebral BMD. There is another histomorphometry study by Laura et al. [100], presenting quite similar results as in our research. Within the study 18 iliac-crest biopsies from T1DM patients and non-diabetic control patients were collected. The results showed that no significant differences were found in anterior-posterior lumbar spine and left hip BMD between T1DM and control groups. Additionally, Tb.Th, BV/TV, Tb.S determined with µCT showed no significant differences between both groups and

histomorphometry data showed osteoid, osteoblast and osteoclast parameters were similar in both groups. Thus, the authors concluded that T1DM had no effect on BMD measured with DXA and bone histomorphometric characteristics of T1DM trabecular bone. Since the studied bone material used in this research was from iliac crest which included trabecular bone, it differs from the femoral cortex analysed in our study. Therefore, our conclusion of bone cellular activity changes can only be made on femoral cortical bone rather than other skeletal sites.

From our result, it might imply that T1DM influences bone cellular activity through increasing bone resorption and decreasing osteocyte number and in the end increasing fracture risk, however, without changing BMD. As can be seen from previous research, T1DM is associated with an increased risk of bone fracture. A large prospective nurse study has reported that hip fractures in female patients with T1DM women patients was six-fold higher than non-diabetic women [77]. A population-based cohort study found elevated hip fracture risk in both men and women with T1DM [101]. Besides the hip as frequent fracture site in T1DM, increased fracture risk in vertebrae has also been reported but less research has been performed yet. [102, 103]. One study showed that, asymptomatic vertebrae fractures were elevated in T1DM patients [78]. Another study found two-fold higher spinal fracture risk [104]. Thus, T1DM has a negative effect on bone, which increases fracture risk.

Why is this increasing resorption accompanied by normal BMD values? In other studies, despite of lower BMD in T1DM patients, such modestly lower BMD is still not enough to explain such a high fracture risk which means high fracture risk can only partially be explained by the reduction of BMD. Other aspects such as bone macro- or microstructural changes including bone remodelling should also be considered in T1DM when performing bone fracture risk assessment. Our study aims to determine BMD in vertebrae and bone remodelling in cortical bone in T1DM patients to link BMD to cellular activity. Since BMD is based on bone remodelling, where activity of bone-building osteoblasts and bone-resorbing osteoclasts are coupled, cellular activity changes are quicker than BMD value decreases in T1DM patients. In addition, insulin treatment might be another aspect that influences bone remodelling processes. This was also proved by other studies that identified insulin was vital in bone remodelling and energy metabolism in a mice research [105]. Insulin can affect bone remodelling by stimulating osteoblast differentiation to increase osteocalcin production which then stimulates more insulin secreted by pancreas [105-107]. Thus, T1DM might have a

negative effect on bone cellular activity that embrittle bone more than influencing bone quantity.

5.2 Concluding hypothesis

These results can be used to explain the hypothesis which we proposed at the beginning. From the results, we can conclude that no obvious difference is found in BMD of 11th thoracic - 1st lumbar vertebrae in T1DM and non-diabetic individuals. We find that bone resorption increases while osteocyte number decreases in T1DM comparing to non-diabetics in femoral mid-diaphyseal anterior bone. However, the combination of normal BMD and increased resorption cannot fully explain high fracture risk in T1DM patients. This might be due to other factors that may contribute to the increased fracture risk in T1DM patients. First, the usage of insulin or other medications might play an important role in preventing bone loss and failure in bone quality. Second, the average age of the samples in our study was 48 years, which means younger age of T1DM patients might be another factor that obtains better bone quality than elderly aged T1DM patients. Third, high fracture risk has been reported in other studies focusing on femoral neck which contains both cortical and trabecular bone while our study has measured femoral mid-diaphysis with only cortical bone. Thus, the duration of the disease, medication and fracture history, and different bone sites are all important to T1DM bone analysis and need to be considered properly in future research.

5.3 Strength of the study

Ex vivo DXA measurement of vertebrae with a water phantom is an innovative method to determine BMD post mortem which has not been widely used [108]. The principle of this measurement is the same as the standard phantom calibration of DXA machine provided by the manufacturer. By this BMD measurement can be performed on samples obtained during autopsy, and provides an important method to analyse bone quality *ex vivo.* Bohnert et al. [109] used the plastic container filled with small plastic beads while Vom Scheidt et al. [108] used polyethylene container filled with

saline solution. In our study, we followed the method in Vom Scheidt's research [108]. Meanwhile, in the presented approach for histomorphometry, we differentiated three different regions within the anterior quadrant: endo-cortical, intra-cortical, and peri-cortical. Since there might be differences in mechanism of bone remodelling due to different regions within the thickness of the femoral cross-section, endo-cortical, intra-cortical, and peri-cortical regions should be measured separately in order to assess different mechanisms in bone remodelling of Control and T1DM femoral mid-cortex. Among these three regions, endo-cortical, which is close to bone marrow, has a bigger area exposed to blood and cells than intra-cortical and peri-cortical bone. Thus, peri-cortical bone remodelling is much lower than that in endo-cortical region [110]. Bone remodelling of endo-cortical region results in cortical bone loss while peri-cortical region make apposition to account for missing endo-cortical bone [111]. On the contrary, remodelling of intra-cortical bone starts within intracortical osteons caused by dynamic loading and increases in fatigue-damaged regions [112]. Therefore, our study used the segmentation method of three equal area of endo-, intra-, and peri-cortical regions to analyse different remodelling patterns in these three different regions. From the result, we could also see that eroded surface is more presented in endo-cortical regions than peri-cortical regions. This might prove that the segmentation method presented in this study is meaningful.

The present study uses two kinds of sample preparation methods for histomorphometry assessment in order to analyse cortical bone. Thin sections are cut to 4 μm thickness while ground sections are grinded to 80 μm thickness. Difference between these two methods due to different thickness are shown. Thin sections facilitate identification of cells compared to ground sections because of no cells overlapping in different layers. However, cracks and tissue overlapping are inevitable during thin section cutting and stretching procedures. On the contrary, cracking and overlapping of bone tissue can be avoided by preparing grinded sections. Nevertheless, bone cells are overlapped in different layers on account of the depth of grinded sections which need to be considered when analysing. Additionally, due to the thickness of the section, black-coloured cells which look like osteocytes are visible in ground sections. The reason of appearance of the black-coloured cells might be that lacunae in a deeper layer of the section are filled with Toluidine Blue dyeing liquor. Thus, it is obvious that thin sections are a better sample preparation to measure bone cells and the border while ground sections are better for area measurements. The combination of these two

methods can provide a better quality in cortical bone histomorphometry assessment. From data comparison of thin and ground sections, we have found difference in N.Ot, N.EmLa and eroded surface. This might attribute to the difference between these two methods mentioned above. Both methods are good and reliable while ground section assessment is more difficult than thin section. A good performance of osteocytes and black-coloured cells differentiation in deeper layer is always needed when performing histomorphometry assessment on grinded sections.

5.4 Limitation of the study

There are also some limitations in this study. Due to the origin of the material obtained during autopsy, sample information is limited and data on diabetes duration, glycaemic control, medication or health care is unknown. Additionally, further information on fracture history cannot be obtained. Furthermore, comorbidities and complications which could increase the risk of falls related to diabetes fracture such as neuropathy or vision impairment are unknown [113]. Small sample size is another limitation of this study due to small number of T1DM patients. Further studies should be proceeded on bone quality in order to identify reasons that cause high fracture risk. However, our study is irreplaceable at some points. Our study provides histomorphometry data on femoral bone samples which were carefully extracted during autopsy. Therefore, we have obtained cortical bone with intact osteons as basic structural units for cortical bone remodelling transversely aligned and from the same skeletal site. Furthermore, we have chosen the experiment method as *ex vivo* DXA and histomorphometry analysis in order to analyse bone density and related cellular activity. Finally, we have applied bone segmentation method to provide bone remodelling analysis in a more precise manner. To conclude, this study presents bone mineral density and cellular activity in human cortical bone afflicted with T1DM and age-matched Controls and provides new insight into bone quality in T1DM patients.

5.5 Outlook

In this study, we confirm that BMD of 11th thoracic to 1st lumbar vertebrae is similar in T1DM compared to non-diabetic individuals while bone resorption is higher and osteocyte number is lower in T1DM. Our study supposes that medication in T1DM might be useful in enhancing bone material quality. However, there are some other questions that remain to be answered. For example, how is the cellular activity of femoral neck in T1DM characterized? Is the bone remodelling process synchronized in different regions, such as vertebrae and femur mid-diaphysis, of the same T1DM individual? What kind of bone parameters could fully explain the high fracture risk in T1DM patients? Since less studies are focusing on bone histomorphometry except one iliac crest biopsy research and our study, more studies are required to validate cellular activity of cortical and trabecular bone in T1DM patients. Meanwhile, the combination of clinical research and *ex vivo* basic experiments might bridge the gap between clinical and basic studies. Thus, better clinical supervision and treatment guidance could be obtained from bone quality assessment in T1DM patients. Future research should not only take into account bone mineral density but also consider macro- and microstructural changes together with complications that relate to falls or muscle weakness of T1DM [114]. Experiments analysing sclerostin levels, hardness, and collagen properties of T1DM bone could also be considered to investigate the original reason of high fracture risk in T1DM patients.

6 Summary

6.1 Summary (English version)

T1DM, characterized by insulin deficiency, is an endocrine disease which presents with higher fracture risk in hip joint and vertebrae but with normal or slightly low BMD value. In order to explain this phenomenon, analysis in bone remodelling activity including bone-resorbing osteoclasts and bone-building osteoblasts which are related to BMD value might be important. Thus, in our study we collected femoral mid-diaphysis and vertebrae from T1DM patients and non-diabetic individuals during autopsy following DXA measurement of vertebrae and histomorphometry analysis of femoral bone.

The study has applied *ex vivo* DXA measurement on vertebrae and adopted two different methods to analyse cortical bone via histomorphometry. Additionally, the anterior quadrant is divided into three regions (endo-cortical, intra-cortical, and peri-cortical) for the ground section in order to analyse cellular activity in a more detailed approach. Similar histomorphometry results were obtained from thin and ground sections. The results for DXA analysis show that 11th thoracic - 1st lumbar vertebrae BMD values are equal in Control and T1DM groups while histomorphometry data reveals that bone resorption is higher and osteocyte number is lower in T1DM group. This study links the quantified values for BMD to cellular activity in non-diabetic individuals and individuals afflicted with T1DM. Our study is an irreplaceable research which provides new data for the research of bone material quality of patients with T1DM.

Further studies of cortical and trabecular bone quality including sclerostin level, bone hardness together with collagen properties in T1DM patients are needed to clarify the mechanism of high fracture risks in T1DM patients.

6.2 Zusammenfassung (Deutsche Version)

T1DM, gekennzeichnet durch Insulinmangel, ist eine endokrine Erkrankung, die ein höheres Frakturrisiko im Hüftgelenk und in den Wirbeln aufweist, jedoch einen normalen oder leicht niedrigen BMD-Wert aufweist. Um dieses Phänomen zu erklären, könnte eine Analyse der Knochenumbauaktivität einschließlich knochenresorbierender Osteoklasten und knochenbildender Osteoblasten, die mit dem BMD-Wert zusammenhängen, wichtig sein. Daher haben wir in unserer Studie während der Autopsie nach DXA-Messung der Wirbel und Histomorphometrieanalyse des Femurknochens femorale Mitteldiaphysen und Wirbel von T1DM-Patienten und Nicht-Diabetikern gesammelt.

Die Studie wendete eine *Ex vivo* DXA-Messung an Wirbeln an und verwendete zwei verschiedene Methoden zur Analyse des kortikalen Knochens mittels Histomorphometrie. Zusätzlich wurde der vordere Quadrant für den Bodenabschnitt in drei Regionen (endokortikal, intrakortikal und perikortikal) unterteilt, um die Zellaktivität in einem detaillierteren Ansatz zu analysieren. Ähnliche histomorphometrische Ergebnisse wurden mit ultradünnen und Bodenschnitten erhalten. Die Ergebnisse für die DXA-Analyse zeigten, dass die BMD-Werte des 11. Brustwirbels - 1. Lendenwirbels in Kontroll- und T1DM-Gruppen gleich waren, während Histomorphometriedaten eine geringe zelluläre Aktivität von Osteoblasten und Osteoklasten in beiden Gruppen zeigten. Die Osteozytendichte sowie der Anteil leerer Lücken waren in beiden Gruppen ähnlich. Obwohl die Studie keinen Unterschied in den BMD- und Histomorphometriedaten in T1DM- und Kontrollgruppen zeigte, verknüpft sie die quantifizierten Werte für BMD mit der Zellaktivität bei nicht-diabetischen Personen und Personen, die an T1DM leiden. Unsere Studie ist eine unersetzliche Studie, die neue Daten für die Untersuchung der Knochenmaterialqualität von Patienten mit T1DM liefert.

Weitere Studien zur kortikalen und trabekulären Knochenqualität, einschließlich Sklerostinspiegel, Knochenhärte und Kollageneigenschaften bei T1DM-Patienten, sind erforderlich, um den Mechanismus hoher Frakturrisiken bei T1DM-Patienten zu klären.

7 Abbreviation

BV/TV	Bone volume per total volume
Tb.N	Trabecular number
Tb.Sp	Trabecular separation
Tb.Th	Trabecular thickness
DM	Diabetes mellitus
T1DM	Type 1 diabetes mellitus
T2DM	Type 2 diabetes mellitus
DXA	Dual-energy X-ray absorptiometry
BMD	Bone mineral density
PBS	Phosphate-buffered saline
PFA	Paraformaldehyde
AP	Anterior-posterior
ROI	Region of Interest
PMMA	Polymethyl Methylmethacrylat
N.Ot/B.Ar	Number of osteocytes per bone area
N.EmLa/B.Ar	Number of empty lacunae per bone area
N.Ot/Tt.No	Number of osteocytes per total number of lacunae
BS/BV	Bone surface per bone volume
B.Ar/T.Ar	Bone area per total area
ES/BS	Eroded surface with osteoclast perimeter per bone surface
Oc.S/BS	Osteoclast surface per bone surface
N.Oc/BS	Number of osteoclasts per bone surface
Ob.S/BS	Osteoblast surface per bone surface
N.Ob/BS	Number of osteoblasts per bone surface
O.Ar/B.Ar	Osteoid area per bone area
OS/BS	Osteoid surface per bone surface
O.Th	Osteoid thickness
Ad.Ar/Tt.Ar	Adipocyte area per total marrow area
N.Ad/Tt.Ar	Number of adipocytes per total marrow area
Ad.D	Adipocyte diameter
Ad.P/N.Ad	Adipocyte perimeter per number of adipocytes
SD	Standard deviation

8 Appendix

Infiltration I (24 hours 4℃ in refrigerator)

1000ml destabilized MMA (Merck 8.00590)

3.3g dried Benzoyl Peroxide (BPO)

100ml Nonylphenol

Infiltration II (24 hours 4℃ in refrigerator)

1000ml destabilized MMA (Merck 8.00590)

3.3g dried BPO (Merck 801641)

100ml Nonylphenol Polyglycolaether Acetate

Embedding Solution

Mixed solution: 1020ml MMA, 6.6g BPO, 80ml Nonylphenol

N,N Dimethyl-p-Toluidin (DMTP) : Mixed solution (1000µl: 200ml)

9 References

[1] Morgan EF, Barnes GL, Einhorn TA. The Bone Organ System: Form and Function. In: Marcus R, Feldman D, Nelson DA, Rosen CJ, editors. Osteoporosis (Third Edition). San Diego: Academic Press; 2008, p. 3-25.

[2] Cooper DML, Kawalilak CE, Harrison K, Johnston BD, Johnston JD. Cortical Bone Porosity: What Is It, Why Is It Important, and How Can We Detect It? Curr Osteoporos Rep 2016;14: 187-98.

[3] Jowsey J. Cortical and Trabecular Bone. In: The Bone Biopsy. Boston, MA: Springer US; 1977, p. 51-58.

[4] Ott SM. Cortical or Trabecular Bone: What's the Difference? Am J Nephrol 2018;47: 373-375.

[5] Parfitt AM. Misconceptions (2): turnover is always higher in cancellous than in cortical bone. Bone 2002;Vol.30, No. 6: 807-809.

[6] Oftadeh R, Perez-Viloria M, Villa-Camacho JC, Vaziri A, Nazarian A. Biomechanics and mechanobiology of trabecular bone: a review. J Biomech Eng 2015;137: 010802-1-15.

[7] Manske SL, Liu-Ambrose T, Cooper DM, Kontulainen S, Guy P, Forster BB, McKay HA. Cortical and trabecular bone in the femoral neck both contribute to proximal femur failure load prediction. Osteoporos Int 2009;20: 445-53.

[8] Chen H, Zhou X, Fujita H, Onozuka M, Kubo KY. Age-related changes in trabecular and cortical bone microstructure. Int J Endocrinol 2013;2013: 213234.

[9] Ritzel H, Amling M, Posl M, Hahn M, Delling G. The thickness of human vertebral cortical bone and its changes in aging and osteoporosis: a histomorphometric analysis of the complete spinal column from thirty-seven autopsy specimens. J Bone Miner Res 1997;12: 89-95.

[10] Roux JP, Wegrzyn J, Arlot ME, Guyen O, Delmas PD, Chapurlat R, Bouxsein ML. Contribution of trabecular and cortical components to biomechanical behavior of human vertebrae: an ex vivo study. J Bone Miner Res 2010;25: 356-61.

[11] Eswaran SK, Gupta A, Adams MF, Keaveny TM. Cortical and trabecular load sharing in the human vertebral body. J Bone Miner Res 2006;21: 307-14.

[12] Christiansen BA, Kopperdahl DL, Kiel DP, Keaveny TM, Bouxsein ML. Mechanical contributions of the cortical and trabecular compartments contribute to differences

in age-related changes in vertebral body strength in men and women assessed by QCT-based finite element analysis. J Bone Miner Res 2011;26: 974-83.

[13] Ruyssen-Witrand A, Gossec L, Kolta S, Dougados M, Roux C. Vertebral dimensions as risk factor of vertebral fracture in osteoporotic patients: a systematic literature review. Osteoporos Int 2007;18: 1271-8.

[14] Chen H, Shoumura S, Emura S, Bunai Y. Regional variations of vertebral trabecular bone microstructure with age and gender. Osteoporos Int 2008;19: 1473-1483.

[15] Gong H, Zhang M, Yeung H, Qin L. Regional variations in microstructural properties of vertebral trabeculae with aging. J Bone Miner Metab 2005;23: 174-180.

[16] Mosekilde L. The effect of modelling and remodelling on human vertebral body architecture. Technol Health Care 1998;6: 287-97.

[17] Green JO, Nagaraja S, Diab T, Vidakovic B, Guldberg RE. Age-related changes in human trabecular bone: Relationship between microstructural stress and strain and damage morphology. J Biomech 2011;44: 2279-85.

[18] Rachner TD, Khosla S, Hofbauer LC. Osteoporosis: now and the future. Lancet 2011;377: 1276-87.

[19] Wasnich RD. Vertebral fracture epidemiology. Bone 1996;18: 179s-183s.

[20] Thomsen JS, Jensen MV, A.S. N, Ebbesen EN, Brüel A. Age-related changes in vertebral and iliac crest 3D bone microstructure--differences and similarities. Osteoporos Int 2015;26: 219-228.

[21] Parfitt AM, Mathews CH, Villanueva AR, Kleerekoper M, Frame B, Rao DS. Relationships between surface, volume, and thickness of iliac trabecular bone in aging and in osteoporosis. Implications for the microanatomic and cellular mechanisms of bone loss. J Clin Invest 1983;72: 1396-409.

[22] Motley RJ, Crawley EO, Evans C, Rhodes J, Compston JE. Increased rate of spinal trabecular bone loss in patients with inflammatory bowel disease. Gut 1988;29: 1332-6.

[23] Mohsin S, Kaimala S, Sunny JJ, Adeghate E, Brown EM. Type 2 Diabetes Mellitus Increases the Risk to Hip Fracture in Postmenopausal Osteoporosis by Deteriorating the Trabecular Bone Microarchitecture and Bone Mass. J Diabetes Res 2019;2019: 3876957.

[24] Chang CY, Rosenthal DI, Mitchell DM, Handa A, Kattapuram SV, Huang AJ. Imaging Findings of Metabolic Bone Disease. Radiographics 2016;36: 1871-1887.

[25] Bajwa NM, Sanchez CP, Lindsey RC, Watt H, Mohan S. Cortical and trabecular bone are equally affected in rats with renal failure and secondary hyperparathyroidism. BMC Nephrol 2018;19: 24.

[26] Iseri K, Qureshi AR, Dai L, Ripsweden J, Heimburger O, Barany P, Bergstrom I, Stenvinkel P, Brismar TB, Lindholm B. Bone mineral density at different sites and 5 years mortality in end-stage renal disease patients: A cohort study. Bone 2020;130: 115075.

[27] Busse B, Bale HA, Zimmermann EA, Panganiban B, Barth HD, Carriero A, Vettorazzi E, Zustin J, Hahn M, Ager JW, 3rd, Puschel K, Amling M, Ritchie RO. Vitamin D deficiency induces early signs of aging in human bone, increasing the risk of fracture. Sci Transl Med 2013;5: 193ra88.

[28] Alho A, Hoiseth A, Husby T. Bone-mass distribution in the femur. A cadaver study on the relations of structure and strength. Acta Orthop Scand 1989;60(1): 101-104.

[29] Ito M, Nishida A, Koga A, Ikeda S, Shiraishi A, Uetani M, Hayashi K, Nakamura T. Contribution of trabecular and cortical components to the mechanical properties of bone and their regulating parameters. Bone 2002;31: 351-358.

[30] Holzer G, Skrbensky VG, Holzer AL, Pichl W. Hip fractures and the contribution of cortical versus trabecular bone to femoral neck strength. J Bone Miner Res. 2009;24: 468-474.

[31] Imamura T, Tsurumoto T. Morphological profile of atypical femoral fractures: age-related changes to the cross-sectional geometry of the diaphysis. J Anat 2019;235(5): 892-902.

[32] Bronx Spine Center - Back Anatomy - Lumbar Vertebrae (L1 - L5) – Bronx, New York. [Online in the Internet.] URL: http://www.bronxspinecenter.com/BACK_ANATOMY.htm. [Status: April 30th, 2020, 06:17pm].

[33] Gregory D. Cramer (2016) Basicmedical Key - General Characteristics of the Spine - Chapter 2. [Online in the Internet.] URL: https://basicmedicalkey.com/general-characteristics-of-the-spine-2/.[Status: April 30th, 2020, 06:17pm].

[34] VectorStock - Femur - Newton, Auckland. [Online in the Internet.] URL: https://www.vectorstock.com/royalty-free-vector/femur-bone-structure-vector-19944594. [Status: April 30th, 2020, 06:17pm].

[35] Bernhard A, Milovanovic P, Zimmermann EA, Hahn M, Djonic D, Krause M, Breer S, Puschel K, Djuric M, Amling M, Busse B. Micro-morphological properties of osteons reveal changes in cortical bone stability during aging, osteoporosis, and bisphosphonate treatment in women. Osteoporos Int 2013;24: 2671-80.

[36] Skedros JG, Holmes JL, Vajda EG, Bloebaum RD. Cement lines of secondary osteons in human bone are not mineral-deficient: new data in a historical perspective. Anat Rec A Discov Mol Cell Evol Biol 2005;286: 781-803.

[37] Ascenzi MG, Ascenzi A, Benvenuti A, Burghammer M, Panzavolta S, Bigi A. Structural differences between "dark" and "bright" isolated human osteonic lamellae. J Struct Biol 2003;141: 22-33.

[38] Fratzl. P, Gupta. HS, Roschger. P, Klaushofer. K. Bone Nanostructure and its Relevance for Mechanical Performance, Disease and Treatment. In: Nanotechnology; 2010, p. 345-360.

[39] Rubin MA, Rubin J, Jasiuk I. SEM and TEM study of the hierarchical structure of C57BL/6J and C3H/HeJ mice trabecular bone. Bone 2004;35: 11-20.

[40] Robles-Linares JA, Ramirez-Cedillo E, Siller HR, Rodriguez CA, Martinez-Lopez JI. Parametric Modeling of Biomimetic Cortical Bone Microstructure for Additive Manufacturing. Materials (Basel) 2019;12.

[41] Zimmermann EA, Busse B, Ritchie RO. The fracture mechanics of human bone: influence of disease and treatment. Bonekey Rep 2015;4: 743.

[42] Kenkre JS, Bassett JHD. The bone remodelling cycle. Ann Clin Biochem 2018;55: 308-327.

[43] Wang J, Zhou B, Liu XS, Fields AJ, Sanyal A, Shi X, Adams M, Keaveny TM, Guo XE. Trabecular plates and rods determine elastic modulus and yield strength of human trabecular bone. Bone 2015;72: 71-80.

[44] Franz-Odendaal TA, Hall BK, Witten PE. Buried alive: how osteoblasts become osteocytes. Dev Dyn 2006;235: 176-190.

[45] Bonewald LF. The amazing osteocyte. J Bone Miner Res 2011;26: 229-38.

[46] Milovanovic P, Busse B. Inter-site Variability of the Human Osteocyte Lacunar Network: Implications for Bone Quality. Curr Osteoporos Rep 2019;17: 105-115.

[47] Santos A, Bakker AD, Klein-Nulend J. The role of osteocytes in bone mechanotransduction. Osteoporos Int 2009;20: 1027-31.

[48] Burr DB, Turner CH, Naick P, Forwood MR, Ambrosius W, Hasan MS, Pidaparti R. Does microdamage accumulation affect the mechanical properties of bone? J Biomech 1998;31: 337-45.

[49] Vashishth D, Verborgt O, Divine G, Schaffler MB, Fyhrie DP. Decline in osteocyte lacunar density in human cortical bone is associated with accumulation of microcracks with age. Bone 2000;26: 375-80.

[50] Milovanovic P, Zimmermann EA, Hahn M, Djonic D, Puschel K, Djuric M, Amling M, Busse B. Osteocytic canalicular networks: morphological implications for altered mechanosensitivity. ACS Nano 2013;7: 7542-51.

[51] Bonewald L. Osteocytes as multifunctional cells. J Musculoskelet Neuronal Interact 2006;6: 331-3.

[52] Liu F, Malaval L, Aubin JE. The mature osteoblast phenotype is characterized by extensive plasticity. Exp Cell Res. 1997;232: 97-105.

[53] Manolagas SC. Birth and death of bone cells: basic regulatory mechanisms and implications for the pathogenesis and treatment of osteoporosis. Endocr Rev 2000;21: 115-37.

[54] Hauge EM, Qvesel D, Eriksen EF, Mosekilde L, Melsen F. Cancellous bone remodeling occurs in specialized compartments lined by cells expressing osteoblastic markers. J Bone Miner Res 2001;16: 1575-82.

[55] Boyle WJ, Simonet WS, Lacey DL. Osteoclast differentiation and activation. Nature 2003;423: 337-42.

[56] Ross FP. Osteoclast Biology and Bone Resorption. In: Primer on the Metabolic Bone Diseases and Disorders of Mineral Metabolism; 2013, p. 25-33.

[57] de Paula FJA, Rosen CJ. Structure and Function of Bone Marrow Adipocytes. Compr Physiol 2017;8: 315-349.

[58] Li Y, Meng Y, Yu X. The Unique Metabolic Characteristics of Bone Marrow Adipose Tissue. Front Endocrinol (Lausanne) 2019;10: 69.

[59] Grabowski P. Physiology of bone. In: Calcium and Bone Disorders in Childern and Adolescents. 2 ed; 2015, p. 33-55.

[60]Seeman E. Bone modeling and remodeling. Crit Rev Eukaryot Gene Expr 2009;19: 219-33.

[61] Allen MR, Burr DB. Chapter 4 - Bone Modeling and Remodeling. In: Burr DB, Allen MR, editors. Basic and Applied Bone Biology. San Diego: Academic Press; 2014, p. 75-90.

[62] Sims NA, Vrahnas C. Regulation of cortical and trabecular bone mass by communication between osteoblasts, osteocytes and osteoclasts. Archives of Biochemistry and Biophysics 2014;561: 22-28.

[63] Parfitt AM. Chapter 15 - Skeletal Heterogeneity and the Purposes of Bone Remodeling: Implications for the Understanding of Osteoporosis. In: Marcus R, Feldman D, Kelsey J, editors. Osteoporosis (Second Edition). San Diego: Academic Press; 2001, p. 433-447.

[64] Delmas PD. Biochemical markers of bone turnover. J Bone Miner Res 1993;8: S549-S555.

[65] Melton LJ, 3rd, Khosla S, Atkinson EJ, O'Fallon WM, Riggs BL. Relationship of bone turnover to bone density and fractures. J Bone Miner Res 1997;12: 1083-91.

[66] Mosekilde L. Consequences of the remodelling process for vertebral trabecular bone structure: a scanning electron microscopy study (uncoupling of unloaded structures). Bone Miner 1990;10: 13-35.

[67] Shah VN, Carpenter RD, Ferguson VL, Schwartz AV. Bone health in type 1 diabetes. Curr Opin Endocrinol Diabetes Obes 2018;25: 231-236.

[68] Ogurtsova K, da Rocha Fernandes JD, Huang Y, Linnenkamp U, Guariguata L, Cho NH, Cavan D, Shaw JE, Makaroff LE. IDF Diabetes Atlas: Global estimates for the prevalence of diabetes for 2015 and 2040. Diabetes Res Clin Pract 2017;128: 40-50.

[69] Rubin MR. Skeletal fragility in diabetes. Ann N Y Acad Sci 2017;1402: 18-30.

[70] Ferrannini E. Insulin resistance versus insulin deficiency in non-insulin-dependent diabetes mellitus: problems and prospects. Endocr Rev 1998;19: 477-90.

[71] American Diabetes Associaton. (2) Classification and diagnosis of diabetes. Diabetes Care 2017;40: S11-S24.

[72] American Diabetes Associaton. Diagnosis and classification of diabetes mellitus. Diabetes Care 2014;37: S81-S90.

[73] Engelgau MM, Geiss LS, Saaddine JB, Boyle JP, Benjamin SM, Gregg EW, Tierney EF, Rios-Burrows N, Mokdad AH, Ford ES, Imperatore G, Narayan KM. The evolving diabetes burden in the United States. Ann Intern Med 2004;140: 945-50.

[74] Sellmeyer DE, Civitelli R, Hofbauer LC, Khosla S, Lecka-Czernik B, Schwartz AV. Skeletal Metabolism, Fracture Risk, and Fracture Outcomes in Type 1 and Type 2 Diabetes. Diabetes 2016;65: 1757-66.

[75] Shah VN, Shah CS, Snell-Bergeon JK. Type 1 diabetes and risk of fracture: meta-analysis and review of the literature. Diabet Med 2015;32: 1134-42.

[76] Nicodemus KK, Folsom AR. Type 1 and type 2 diabetes and incident hip fractures in postmenopausal women. Diabetes Care 2001;24: 1192-7.

[77] Janghorbani M, Feskanich D, Willett WC, Hu F. Prospective study of diabetes and risk of hip fracture: the Nurses' Health Study. Diabetes Care 2006;29: 1573-8.

[78] Zhukouskaya VV, Eller-Vainicher C, Vadzianava VV, Shepelkevich AP, Zhurava IV, Korolenko GG, Salko OB, Cairoli E, Beck-Peccoz P, Chiodini I. Prevalence of morphometric vertebral fractures in patients with type 1 diabetes. Diabetes Care 2013;36: 1635-40.

[79] Shah VN, Harrall KK, Shah CS, Gallo TL, Joshee P, Snell-Bergeon JK, Kohrt WM. Bone mineral density at femoral neck and lumbar spine in adults with type 1 diabetes: a meta-analysis and review of the literature. Osteoporos Int 2017;28: 2601-2610.

[80] Pisani P, Renna MD, Conversano F, Casciaro E, Muratore M, Quarta E, Paola MD, Casciaro S. Screening and early diagnosis of osteoporosis through X-ray and ultrasound based techniques. World J Radiol 2013;5: 398-410.

[81] NIH Consensus Development Panel on Osteoporosis Prevention, Diagnosis, and Therapy. Osteoporosis prevention, diagnosis, and therapy. JAMA 2001;285: 785-95.

[82] Lotz JC, Cheal EJ, Hayes WC. Fracture prediction for the proximal femur using finite element models: Part I--Linear analysis. J Biomech Eng 1991;113: 353-60.

[83] Marshall D, Johnell O, Wedel H. Meta-analysis of how well measures of bone mineral density predict occurrence of osteoporotic fractures. BMJ 1996;312: 1254-9.

[84] Lewiecki EM. Update on bone density testing. Curr Osteoporos Rep 2005;3: 136-42.

[85] Lewiecki EM, Lane NE. Common mistakes in the clinical use of bone mineral density testing. Nat Clin Pract Rheumatol 2008;4: 667-74.

[86] Mazess R, Chesnut CH, 3rd, McClung M, Genant H. Enhanced precision with dual-energy X-ray absorptiometry. Calcif Tissue Int 1992;51: 14-7.

[87] Njeh CF, Fuerst T, Hans D, Blake GM, Genant HK. Radiation exposure in bone mineral density assessment. Appl Radiat Isot 1999;50: 215-36.

[88] Carey JJ, Delaney MF. T-Scores and Z-Scores. Clin Rev Bone Miner Metab 2010;8: 113-121.

[89] 123RF – Stock Photo – Male Human Skeleton – Germany. [Online in the Internet.] URL: https://www.123rf.com/photo_11713071_male-human-skeleton-four-views-front-back-side-and-perspective-scientifically-correct-photorealistic.html. [Status: May 1st, 2020, 12:17am].

[90] Nirody JA, Cheng KP, Parrish RM, Burghardt AJ, Majumdar S, Link TM, Kazakia GJ. Spatial distribution of intracortical porosity varies across age and sex. Bone 2015;75: 88-95.

[91] Heilmeier U, Cheng K, Pasco C, Parrish R, Nirody J, Patsch JM, Zhang CA, Joseph GB, Burghardt AJ, Schwartz AV, Link TM, Kazakia G. Cortical bone laminar analysis reveals increased midcortical and periosteal porosity in type 2 diabetic postmenopausal women with history of fragility fractures compared to fracture-free diabetics. Osteoporos Int 2016;27: 2791-2802.

[92] Neumann T, Samann A, Lodes S, Kastner B, Franke S, Kiehntopf M, Hemmelmann C, Lehmann T, Muller UA, Hein G, Wolf G. Glycaemic control is positively associated with prevalent fractures but not with bone mineral density in patients with Type 1 diabetes. Diabet Med 2011;28: 872-5.

[93] Ingberg CM, Palmer M, Aman J, Arvidsson B, Schvarcz E, Berne C. Body composition and bone mineral density in long-standing type 1 diabetes. J Intern Med 2004;255: 392-8.

[94] Rakic V, Davis WA, Chubb SA, Islam FM, Prince RL, Davis TM. Bone mineral density and its determinants in diabetes: the Fremantle Diabetes Study. Diabetologia 2006;49: 863-71.

[95] Lunt H, Florkowski CM, Cundy T, Kendall D, Brown LJ, Elliot JR, Wells JE, Turner JG. A population-based study of bone mineral density in women with longstanding type 1 (insulin dependent) diabetes. Diabetes Res Clin Pract 1998;40: 31-8.

[96] Leidig-Bruckner G, Grobholz S, Bruckner T, Scheidt-Nave C, Nawroth P, Schneider JG. Prevalence and determinants of osteoporosis in patients with type 1 and type 2 diabetes mellitus. BMC Endocr Disord 2014;14: 33.

[97] Slade JM, Coe LM, Meyer RA, McCabe LR. Human bone marrow adiposity is linked with serum lipid levels not T1-diabetes. J Diabetes Complications 2012;26: 1-9.

[98] Vestergaard P. Discrepancies in bone mineral density and fracture risk in patients with type 1 and type 2 diabetes--a meta-analysis. Osteoporos Int 2007;18: 427-44.

[99] Pan H, Wu N, Yang T, He W. Association between bone mineral density and type 1 diabetes mellitus: a meta-analysis of cross-sectional studies. Diabetes Metab Res Rev 2014;30: 531-42.

[100] Armas LA, Akhter MP, Drincic A, Recker RR. Trabecular bone histomorphometry in humans with Type 1 Diabetes Mellitus. Bone 2012;50: 91-6.

[101] Miao J, Brismar K, Nyren O, Ugarph-Morawski A, Ye W. Elevated hip fracture risk in type 1 diabetic patients: a population-based cohort study in Sweden. Diabetes Care 2005;28: 2850-5.

[102] Vestergaard P, Rejnmark L, Mosekilde L. Relative fracture risk in patients with diabetes mellitus, and the impact of insulin and oral antidiabetic medication on relative fracture risk. Diabetologia 2005;48: 1292-9.

[103] Starup-Linde J, Hygum K, Harsløf T, Langdahl B. Type 1 Diabetes and Bone Fragility: Links and Risks. Diabetes Metab Syndr Obes 2019;12: 2539-2547.

[104] Jensen MH, Vestergaard P. Hypoglycaemia and type 1 diabetes are associated with an increased risk of fractures. Osteoporos Int 2019;30: 1663-1670.

[105] Ferron M, Wei J, Yoshizawa T, Del Fattore A, DePinho RA, Teti A, Ducy P, Karsenty G. Insulin signaling in osteoblasts integrates bone remodeling and energy metabolism. Cell 2010;142: 296-308.

[106] Torres-Costoso A, Pozuelo-Carrascosa DP, Alvarez-Bueno C, Ferri-Morales A, Miota Ibarra J, Notario-Pacheco B, Martinez-Vizcaino V. Insulin and bone health in young adults: The mediator role of lean mass. PLoS One 2017;12: e0173874.

[107] Klein GL. Insulin and bone: Recent developments. World J Diabetes 2014;5: 14-6.

[108] Vom Scheidt A, Grisolia Seifert EF, Pokrant C, Puschel K, Amling M, Busse B, Milovanovic P. Subregional areal bone mineral density (aBMD) is a better predictor of heterogeneity in trabecular microstructure of vertebrae in young and aged women than subregional trabecular bone score (TBS). Bone 2019;122: 156-165.

[109] Bohnert KL, Gutekunst DJ, Hildebolt CF, Sinacore DR. Dual-energy X-ray absorptiometry of human metatarsals: precision, least significant change and association to ex vivo fracture force. Foot (Edinb) 2013;23: 63-9.

[110] Balena R, Shih MS, Parfitt AM. Bone resorption and formation on the periosteal envelope of the ilium: a histomorphometric study in healthy women. J Bone Miner Res 1992;7: 1475-82.

[111] Compston J. Age-related changes in bone remodelling and structure in men: histomorphometric studies. J Osteoporos 2011;2011: 108324.

[112] Mori S, Burr DB. Increased intracortical remodeling following fatigue damage. Bone 1993;14: 103-9.

[113] Napoli N, Chandran M, Pierroz DD, Abrahamsen B, Schwartz AV, Ferrari SL. Mechanisms of diabetes mellitus-induced bone fragility. Nat Rev Endocrinol 2017;13: 208-219.

[114] Bonjour JP, Ammann P, Rizzoli R. Importance of preclinical studies in the development of drugs for treatment of osteoporosis: a review related to the 1998 WHO guidelines. Osteoporos Int 1999;9: 379-93.

10 Acknowledgements

I would like to acknowledge my tutor Professor Björn Busse, who is always very patient and kind, in involving me as a MD student in the institute of osteology and biomechanics and helping me with this diabetes project. I really appreciate this opportunity and learning experience which are given by Professor Busse.

I would also like to show my heartfelt gratitude to PD Dr. Katharina Jähn and Eva Maria Wölfel for their patiently help in the discussion of the whole project and abstract and thesis writing. They always encouraged me in the process of the learning and doing experiments and really helpful in intriguing my interest into this diabetes project. They also helped me with experiment methods and taught me a lot. Thanks again for their help.

And my cordial thanks to Kilian Stockhausen, who helped me with the segmentation method and encouraged me to try to do ground section. Thanks to Felix Schmidt, Annika vom Scheidt, Imke Fiedler who always kindly gives suggestions during lab meeting discussion. Thanks to Eric Flavio Grisolia Seifert for teaching me and helping me with DXA measurement. Thanks to Maiwulanjiang Mamuti for teaching me the staining part of histomorphometry. Thanks to Michael Hahn and technician Elke Leicht and Andrea for helping me with section making. And thanks to all my colleagues in this institute.

I wound also express my gratitude to Svenja Anderson for helping me with works and dormitory in Hamburg.

Thanks to Southeast University for giving me a good platform.

Last but not least, thanks to my father and mother for supporting me from beginning till now. Thanks to my gracious grandpa and grandma who always give me courage. Thanks to my girlfriend who has waited me for three years.

Thanks to all of you who have helped me when I am abroad. All the best wishes to you!

11 Curriculum Vitae

Lebenslauf wurde aus datenschutzrechtlichen Gründen entfernt.

12 Affidavit (Eidesstattliche Erklärung)

Ich versichere ausdrücklich, dass ich die Arbeit selbständig und ohne fremde Hilfe verfasst, andere als die von mir angegebenen Quellen und Hilfsmittel nicht benutzt und die aus den benutzten Werken wörtlich oder inhaltlich entnommenen Stellen einzeln nach Ausgabe (Auflage und Jahr des Erscheinens), Band und Seite des benutzten Werkes kenntlich gemacht habe.

Ferner versichere ich, dass ich die Dissertation bisher nicht einem Fachvertreter an einer anderen Hochschule zur Überprüfung vorgelegt oder mich anderweitig um Zulassung zur Promotion beworben habe.5

Ich erkläre mich einverstanden, dass meine Dissertation vom Dekanat der Medizinischen Fakultät mit einer gängigen Software zur Erkennung von Plagiaten überprüft werden kann.

Unterschrift: .....Ma Liangyu.....